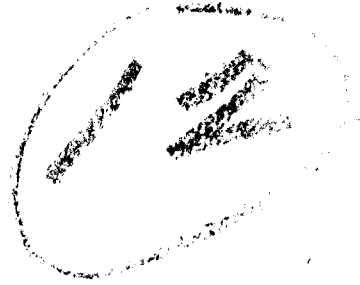


A013424



RIVERSIDE RESEARCH INSTITUTE



Handwritten: 12/23

Best Available Copy

RIVERSIDE RESEARCH INSTITUTE



80 West End Avenue / New York, New York 10023 / (212) 873-4000

31 October 1974

TECHNICAL REPORT T-1/306-3-11
LASER CORRELOGRAPHY: TRANSMISSION OF
HIGH-RESOLUTION OBJECT SIGNATURES
THROUGH THE TURBULENT ATMOSPHERE

By M. Elbaum, M. King and M. Greenebaum

Prepared for

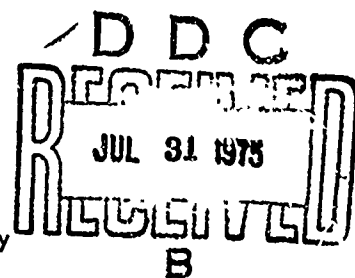
Commanding General
U.S. Army Missile Command
Redstone Arsenal, Alabama 35809

Contract No. DAAH01-74-C-0419

Sponsored by

Advanced Research Projects Agency
Arlington, Virginia 22209

ARPA Order No. 2281



DISTRIBUTION STATEMENT A

Approved for public release/
Distribution Unlimited

RIVERSIDE RESEARCH INSTITUTE

AUTHORIZATION

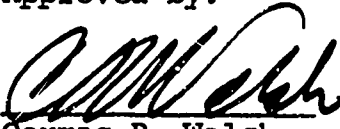
This report describes research performed at Riverside Research Institute and was prepared by M. Elbaum, M. King, and M. Greenebaum.

This project is supported by the Advanced Research Projects Agency of the Department of Defense under Contract No. DAAH01-74-C-0419.

Submitted by:

Marvin King
Manager, Optics
Laboratory

Approved by:


Cormac P. Walsh
Vice President
for Research

RIVERSIDE RESEARCH INSTITUTE

ABSTRACT

A correlogram is the two-dimensional autocorrelation of the image of an object illuminated with non-coherent radiation. A laser correlogram is obtained from the power spectrum of the irradiance pattern scattered from the object when illuminated with sufficiently coherent radiation. The resolution of this signature is dictated by the size of the receiving aperture, with relatively minor degradation by atmospheric turbulence. This report collects in one place information which has been available up to now only in conference proceedings or in limited-circulation Research Notes of the Riverside Research Institute. The subjects treated analytically include: a model for laser backscattering, studies on the influence of atmospheric turbulence on the laser correlogram, statistical convergence properties of the laser correlogram signature, qualitative experimental laboratory results, and the outline of a design for a ruby-laser experiment using space objects.

RIVERSIDE RESEARCH INSTITUTE

TABLE OF CONTENTS

	<u>Page</u>
ABSTRACT	iii
INTRODUCTION	1
PAPER NO. 1: LASER CORRELOGRAPHY SYSTEMS FOR OBTAINING SIGNATURES OF SPACE OBJECTS	4
I. CORRELOGRAPHY--AN OVERVIEW	5
II. ATMOSPHERIC LIMITATIONS	11
III. SYSTEM DESIGN AND IMPLEMENTATION	11
A. WAVELENGTH UTILIZATION	13
B. VISIBLE WAVELENGTH SYSTEM PARAMETERS	16
C. CARBON DIOXIDE SYSTEM PARAMETERS	16
Appendix: LASER ILLUMINATOR ENERGY REQUIREMENTS	24
PAPER NO. 2: INFLUENCE OF THE ATMOSPHERE ON LASER-PRODUCED SPECKLE PATTERNS	26
PAPER NO. 3: LASER-PRODUCED SPECKLE PATTERNS AS SEEN THROUGH A RANDOMLY INHOMOGENEOUS ATMOSPHERE	32
PAPER NO. 4: THE RESIDUAL EFFECTS OF ATMO- SPHERIC TURBULENCE ON A CLASS OF HOLOGRAPHIC IMAGING AND CORRELOGRAPHY SYSTEMS	70
PAPER NO. 5: COMPUTATIONS OF SIGNAL-TO-NOISE RATIO IN CORRELOGRAPHY	85
PAPER NO. 6: PRELIMINARY PLAN FOR A LASER CORRELOGRAPHY EXPERIMENT	93
REFERENCES	113

RIVERSIDE RESEARCH INSTITUTE

INTRODUCTION

Ordinary ground-based imaging of space objects is limited in resolution by atmospheric turbulence to a "seeing" angle of approximately one arc-second ($5 \mu\text{rad}$) under routine clear-air observation conditions. One method of circumventing this "seeing" limitation, laser correlography, can yield object signatures with "diffraction-limited resolution". This Technical Report is a compendium of six papers which go into varying levels of detail on several aspects of laser correlography. Portions of these papers have appeared previously as RRI Research Notes¹⁻⁵ or in conference proceedings^{6,7}.

The "system concept" for obtaining ground-based, diffraction-limited signatures of space objects is as follows (Paper No. 1): The signature is the object correlogram, or two-dimensional autocorrelation of the object radiance in the absence of turbulence. This signature is obtained by laser correlography, the measurement of the power spectrum of the irradiance pattern scattered from an object when it is illuminated with sufficiently coherent radiation, i. e., when it lies well within the coherence volume. Detection of the backscattered intensity across the receiver aperture is employed: a well-corrected receiving telescope is not needed; when fine resolution is desired, a large array of "photon buckets" can be used. In the special case in which a single strong glint point is present on or near an otherwise diffuse target, laser correlography is identical with the well-known on-axis lensless Fourier-transform holographic imaging technique.⁸⁻¹⁰ In the absence of a glint point, a correlogram is obtained, as illustrated in Fig. 4 of Paper No. 1.^{1,11,12} Systems capable of yielding useful signatures in practice are described, and energy requirements

RIVERSIDE RESEARCH INSTITUTE

on the laser illuminator needed for space objects are derived in this paper.

Verification of the basic ideas involved in laser correlography has been accomplished at RRI by a combination of theoretical work and laboratory demonstrations. Paper No. 2 includes a model for laser backscattering, a condensed account of the influence of atmospheric turbulence on the laser correlogram, and some early, qualitative experimental results.⁶ These results, as well as related demonstration experiments performed by others,^{8,9,11-14} are consistent with our calculations.

A fuller account of the reason why laser correlography is insensitive to the effects of atmospheric turbulence is contained in Papers No. 3 and 4. The first of these is based on the Huygens-Fresnel principle and a simplified model of a rough target, and considers an idealized laser illuminator, an exo-atmospheric space object, and a ground-based receiver, with isoplanatism assumed. The effects of using a ground-based illuminator are taken into account in Paper No. 4.⁷ Realistic estimates of the residual effects of atmospheric turbulence, related to scintillation, are given as a function of zenith angle. For slowly rotating space objects of angular subtense less than $10 \mu\text{rad}$, it is concluded that the system concept is valid with CO_2 laser illumination even at large zenith distances if a detector array is employed, and with a visible laser of long coherence length for the object very close to zenith. Verification of the concept over near-horizontal paths is difficult.⁷⁻⁹

The statistical convergence properties of the laser correlogram signature are examined in Paper No. 5, where it is shown that twenty or so independent realizations of the irradiance distribution suffice to obtain adequate signal-to-noise ratio.⁵ This result has been verified in recent demonstration experiments at RRI.¹⁵ (A supplementary Technical Report is in

RIVERSIDE RESEARCH INSTITUTE

preparation¹⁵ which contains the results of recent laboratory demonstrations and computer processing of laser correlograms of diverse objects, including three-dimensional "glinty" ones.)

Based on the component requirements (suggested by Paper No. 1), the statistical convergence properties (developed in Paper No. 5), and the effects of atmospheric turbulence (Papers No. 3 and 4), a feasibility demonstration experiment was designed. This experiment (Paper No. 6) would employ a ruby laser transmitter with a coherence length of 10 meters, operating at a repetition rate of 20 pulses per minute, with an output of 10 joules per 100-nanosecond pulse. A very narrow (5 arc-sec) beamwidth is required. The receiver would employ a SIT or EBS tube preceded by an image intensifier, with the S-25 photocathode located in the plane of the (re-imaged) entrance pupil of the (1.5-m diameter) telescope. A full-fledged system capable of imaging high-altitude space objects would employ a CO₂ laser and a large receiver array, as discussed in Paper No. 1, and in more detail in Ref. 1.

RIVERSIDE RESEARCH INSTITUTE

Paper No. 1

LASER CORRELOGRAPHY SYSTEMS FOR OBTAINING SIGNATURES OF SPACE OBJECTS

(This paper is an edited version of unclassified portions of Research Note N-5/174-3-33, 21 August 1972.¹ The power calculations relate to ensemble-averaged power within a "single speckle". For other (statistical) considerations, see Paper No. 5.)

RIVERSIDE RESEARCH INSTITUTE

LASER CORRELOGRAPHY SYSTEMS FOR OBTAINING SIGNATURES OF SPACE OBJECTS

I. Correlography--An Overview

Correlography is a quasi-imaging process whose output is equal to the autocorrelation function of the target image; this technique may provide length measurement with resolution limited by detection aperture in addition to feature and target recognition. A correlogram system detects the intensity distribution of the backscatter (self-interference) pattern of the target (Fig. 1) and operates on it in the manner shown in Fig. 2.

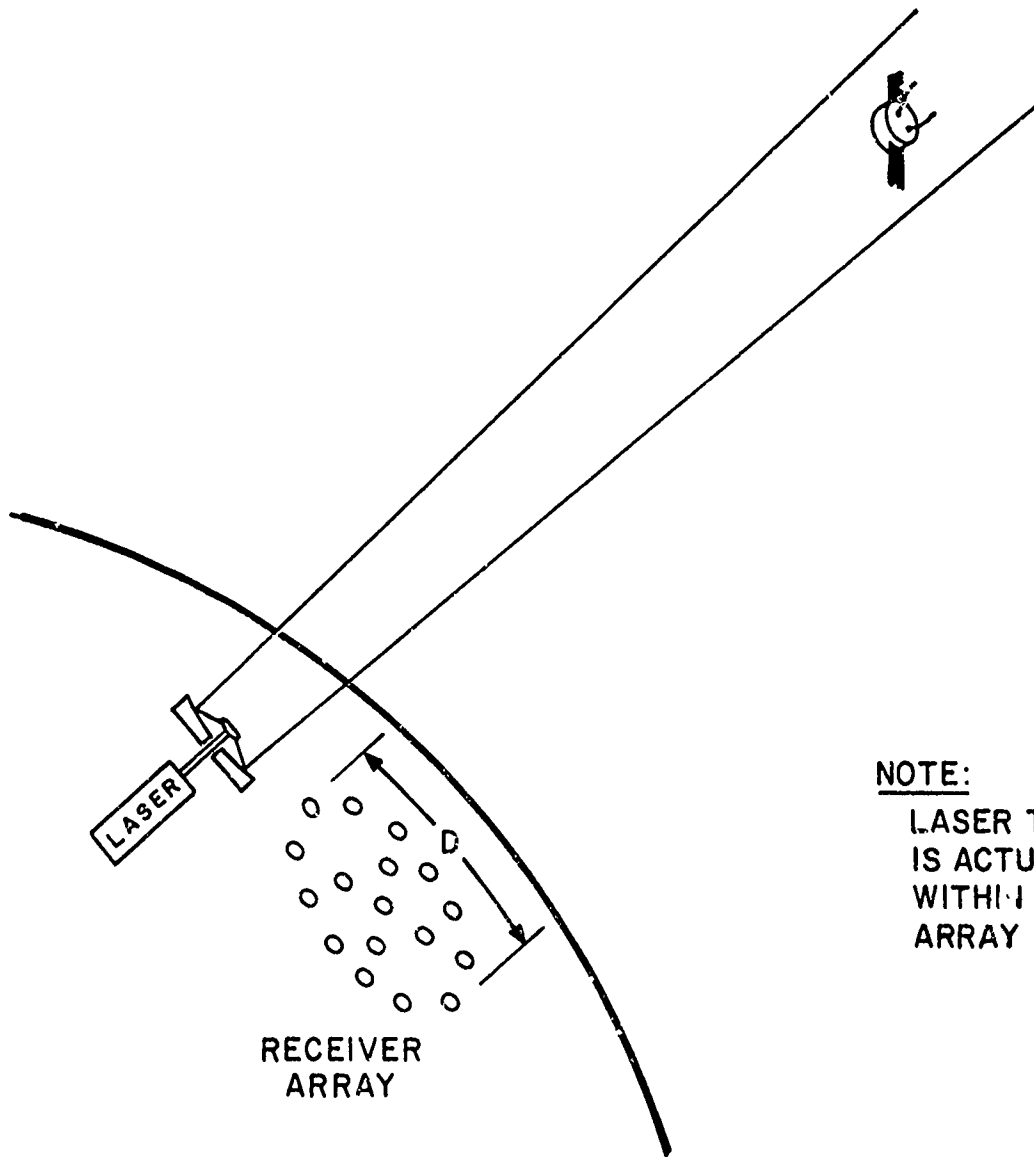
The average intensity of the backscatter pattern is first subtracted from the total signal, then the power spectrum of the residue (speckle component) is computed, followed by a two-dimensional Fourier transform; it has been shown that the resulting two-dimensional distribution is proportional to the image autocorrelation function;¹¹ one may associate with the autocorrelation function a resolution which is limited by the aperture over which the backscatter intensity was detected. Such correlogram systems are, to a large extent, immune to the atmosphere because they operate on backscattered intensity and are therefore phase-insensitive.⁴ The similarity of correlography to holography may be appreciated by noting that if the image consists of a large diffuse area and a bright point (such as that due to a glint) then the correlogram is identical to the on-axis hologram⁸⁻¹⁰.

Using the setup of Fig. 3, correlograms were formed for simple shapes in the laboratory, yielding the results shown in Fig. 4. The top row shows the target images that were used to generate the correlograms; the second row contains the correlograms of the images; the third row contains traces formed by a pinhole detector scanned through the principal axes of the correlograms of the rectangle and T shapes. Several features and properties of correlograms become apparent upon inspection of this figure. First, it is seen that the correlogram offers information along two dimensions which are both transverse to the optical line-of-sight and that these dimensions may yield accurate measurements of lengths of various target features. Secondly, all correlograms have point symmetry, imposing some ambiguity on the patterns; this may make unique target identification difficult in some cases. Finally, the correlograms

RIVERSIDE RESEARCH INSTITUTE

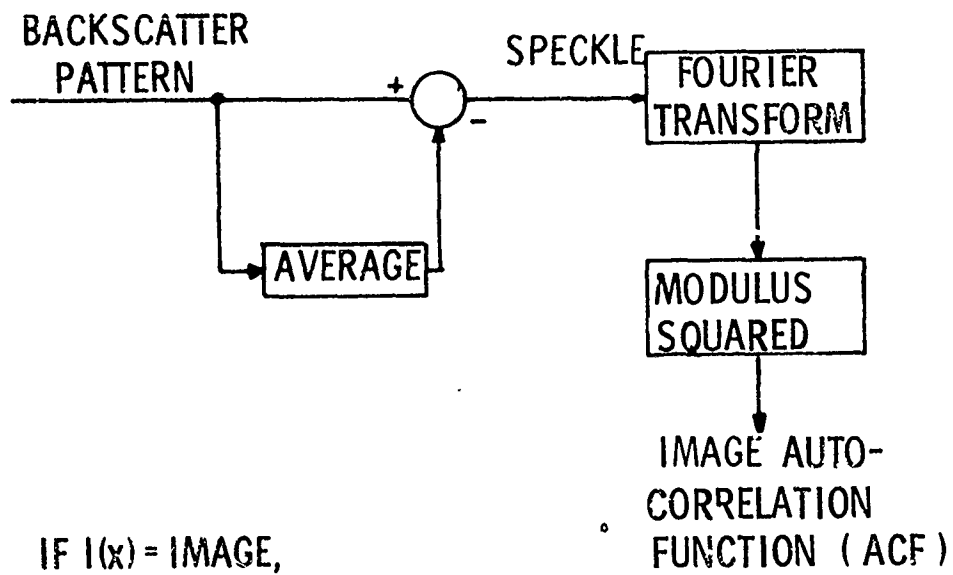
In Fig. 1, the schematic diagram of a ground-based laser system which serves as a model for the discussions of this paper, the relative scales of the laser illuminator and the elements in the receiver array are distorted. Also note that the laser illuminator would typically be placed somewhere within the receiver array. It is implicit throughout the discussion that meteorological conditions permit line-of-sight optical viewing of the space object; no heavy cloud cover, fog, haze, or precipitation is presumed to lie within the path.

FIG. 1 LASER CORRELOGRAPHY SYSTEM



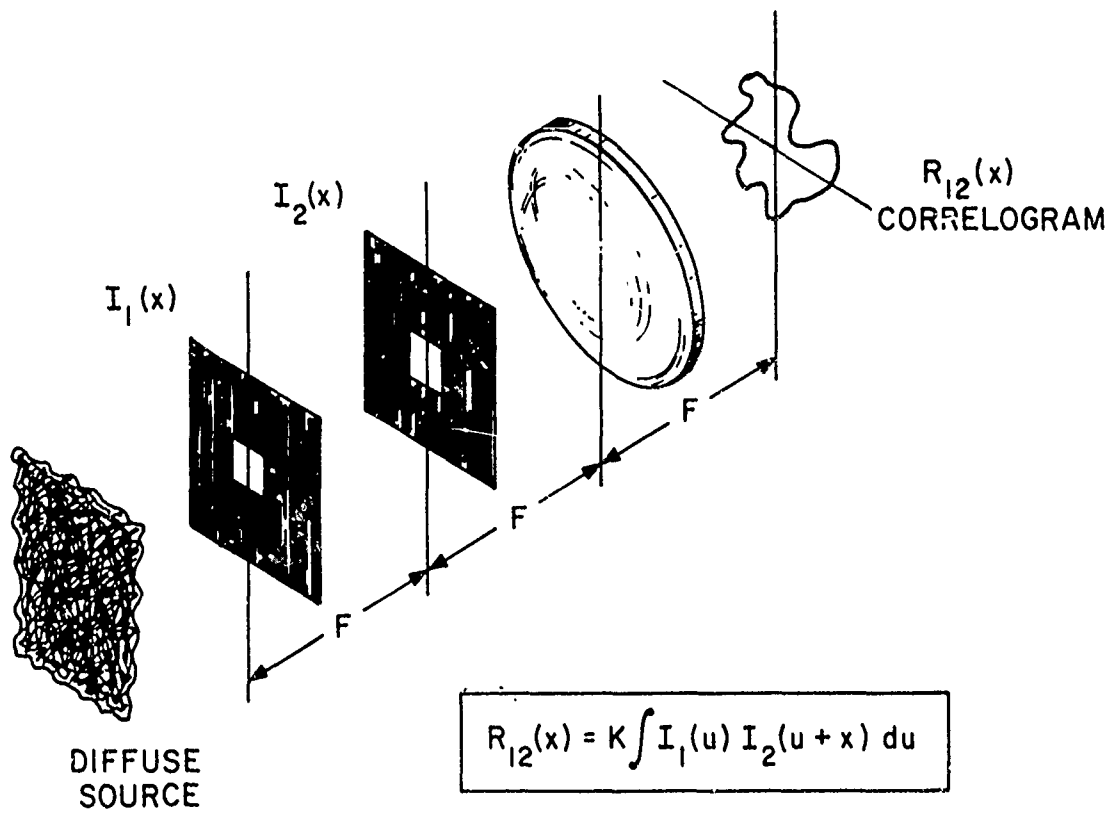
NOTE:
LASER TRANSMITTER
IS ACTUALLY PLACED
WITHIN RECEIVER
ARRAY AREA

FIG. 2 CORRELOGRAPHY



IF $I(x)$ = IMAGE,
 IMAGE ACF = $\int I(x)I(x+u) dx$ = CORRELOGRAM

FIG. 3 OPTICAL CORRELOGRAMS



A-174-3-33-0010

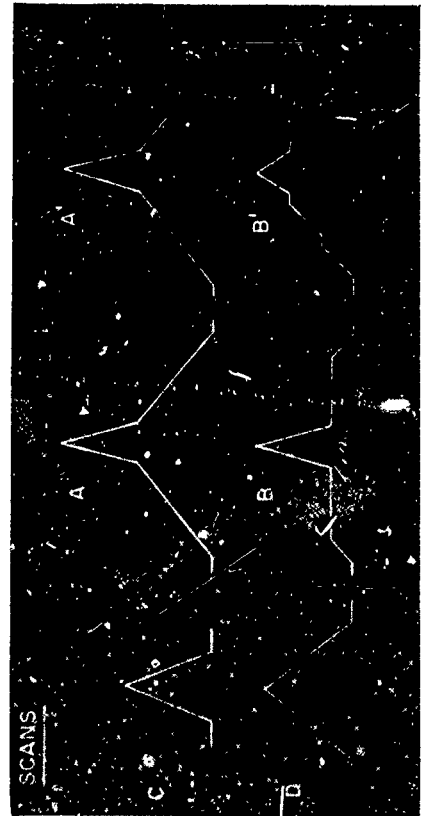
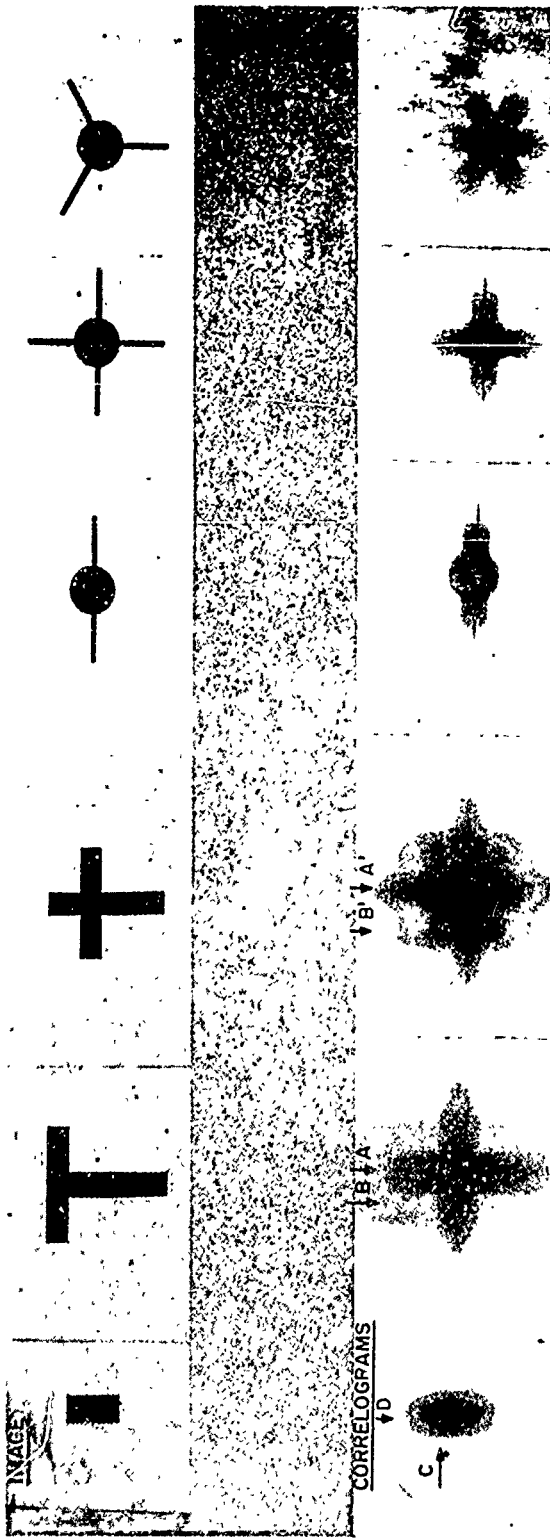


FIG. 4 CORRELOGRAMS

RIVERSIDE RESEARCH INSTITUTE

are observed to preserve angle relationships among paddles, aerials, and other protruding linear structures.

In view of the potential value of these signatures, RRI has made a study of means and rational procedures for information retrieval from correlograms of interesting targets.^{5, 6, 15} This study includes mensuration, feature recognition, target recognition, and image recovery. In addition, laser correlograms have been formed in the laboratory for interesting targets for the purpose of revealing the nature of the degradations caused by such effects as the three-dimensional nature and multiple glint content of typical targets.¹⁵

II. Atmospheric Limitations (See also Papers No. 2, 3, and 4.)

It is known that propagation of a laser illumination beam through the atmosphere to a space object is influenced by the turbulence structure of the atmosphere; in particular, it appears that the beam will break up and this may cause a highly structured illumination to fall on distant targets, resulting in severe fading of the returns.⁷ In addition, the intensity distribution of the backscatter pattern is known to be perturbed by a random apodization due to the atmospheric structure; this random apodization may limit the ultimate resolution of laser backscatter systems, providing an upper limit on useful aperture sizes for receiver arrays.^{3, 4, 6, 7}

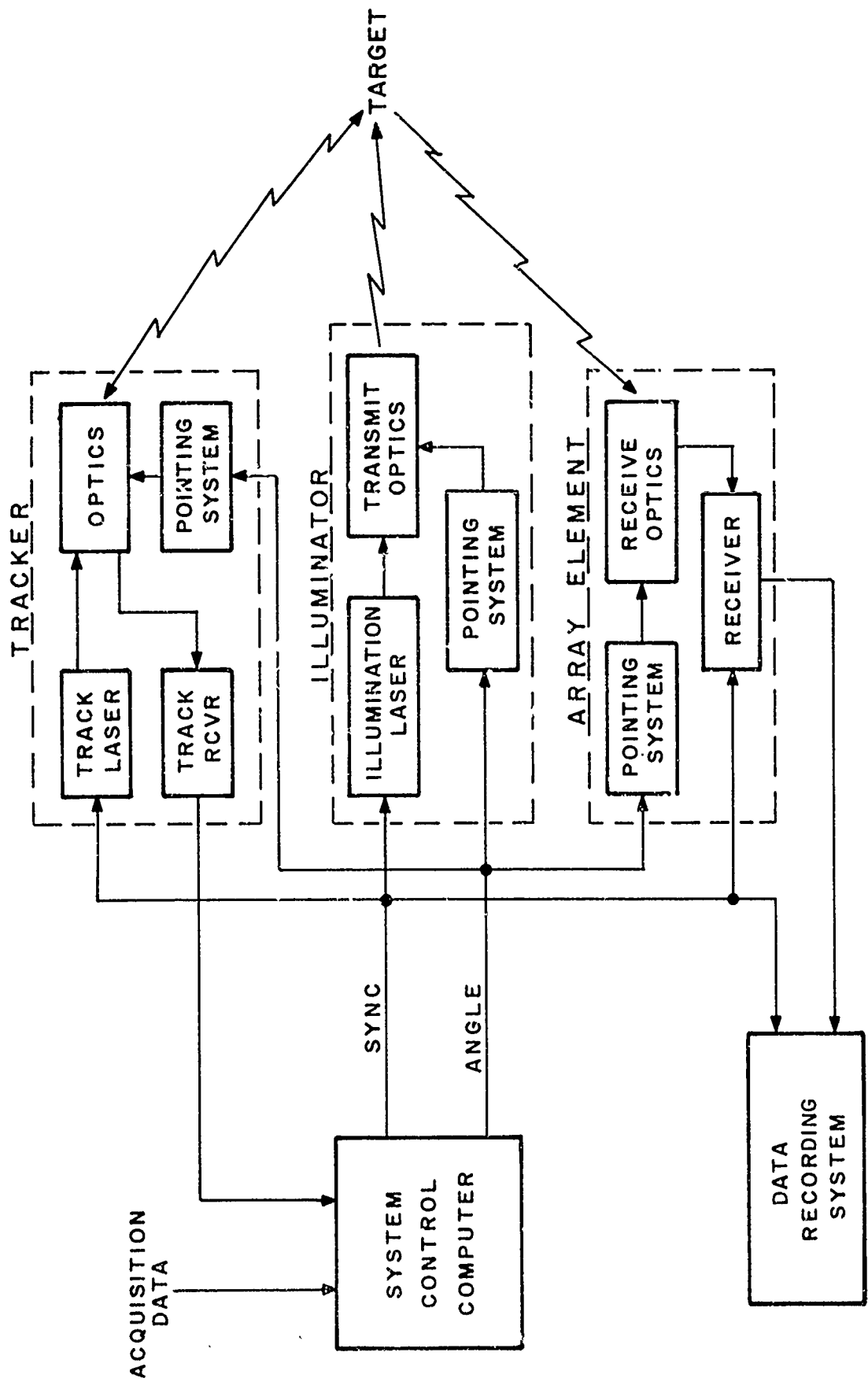
It is recommended that the influence of the atmosphere on target illumination and signature resolution be explored in order to place ultimate limits on performance of laser backscatter systems.²

III. System Design and Implementation

Possessing a general understanding of the signatures offered by laser correlography systems, one can consider the difficulties envisioned in implementing practical operating systems. This section discusses some of the principles and specifications for the selection of the illumination laser, backscatter detection system, target tracking system, and receiver configuration.

The discussion is presented with reference to the general system block diagram shown in Fig. 5. The major elements in the system are the system control computer, tracker, illuminator, array receiver, and data recording system. The system control computer processes coarse acquisition data and fine tracking data in order to point the illumination laser and the array elements; it also provides synchronization of illuminator

FIG. 5 LASER CORRELOGRAPHY SYSTEM BLOCK DIAGRAM



RIVERSIDE RESEARCH INSTITUTE

pulses, receiver range gates, and the data recording system. A separate target tracker is provided to convert the coarse acquisition data (which may have been obtained from an LWIR system) into fine tracks with accuracy on the order of 10 μ rad. The tracker consists of a tracking laser, duplexed transmit/receive optics, an angle and range tracker receiver, and a mechanical pointing system. After an adequately precise track is established, the illumination subsystem directs the illumination laser beam through the transmit optics toward the target; a precision pointing system is required to keep the illumination beam on the target. Backscattered signals are detected by an array of receiver telescopes; each array element consists of a precise pointing system, receiver optics, and a range-gated receiver for detecting the backscattered energy. The data recording system stores all pertinent backscatter signals and system diagnostic data.

A. Wavelength Utilization

In this section, preferred operational wavelengths are established, general design concepts are proposed, and the specification of the illumination and array receiver subsystems are discussed.

Figure 6 compares the "diffraction-limited resolution" (taken as the product of laser wavelength and target range, divided by array aperture length) for ruby and carbon dioxide lasers as a function of receiver aperture size, with target range as a parameter. Note that with ruby laser illumination, a 1.5-meter aperture can yield resolution of 20 cm for 400-km target range and 50 cm on 1,000-km targets; carbon dioxide systems with like resolution would require apertures of 20 m and 50 m, respectively. For 10,000 km target range, a CO₂ laser correlography system requires an aperture of 400 m in order to obtain resolution of 40 cm on a target; proportionally larger apertures are required for synchronous altitudes. It is concluded that it appears more practical to employ visible laser wavelengths in order to reduce the large aperture requirements associated with carbon dioxide systems.

However, Fig. 7 compares ruby and carbon dioxide transmitter energy requirements as a function of the number of photons received per spatial resolution cell in the backscatter pattern for altitudes up to several thousand kilometers. (The derivation of these curves is given in the Appendix.) It is easily observed that visible lasers require much more transmitter energy to yield the same number of photons in the receiver. (It is shown in the Appendix that, at low altitudes, the required laser energy is proportional to the cube of the optical

FIG. 6 RESOLUTION VS APERTURE SIZE FOR TWO WAVELENGTHS

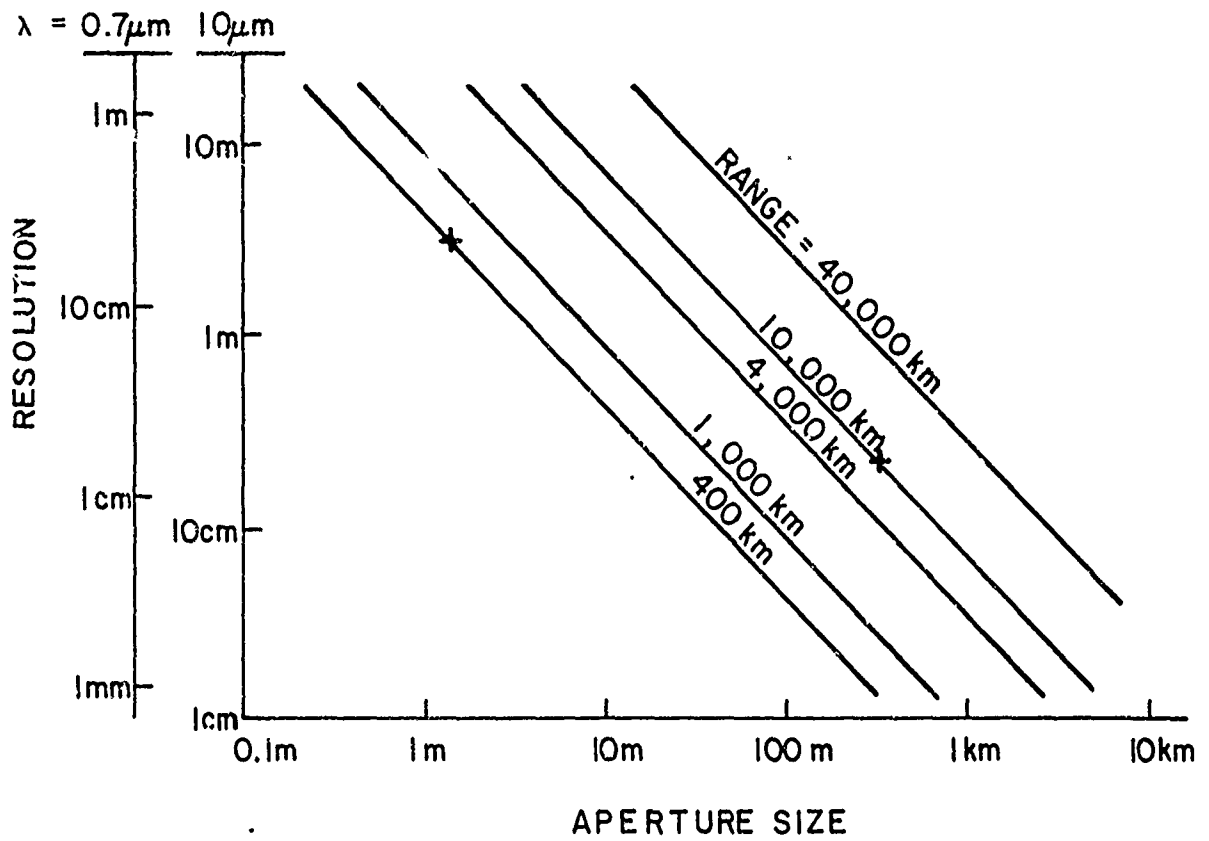
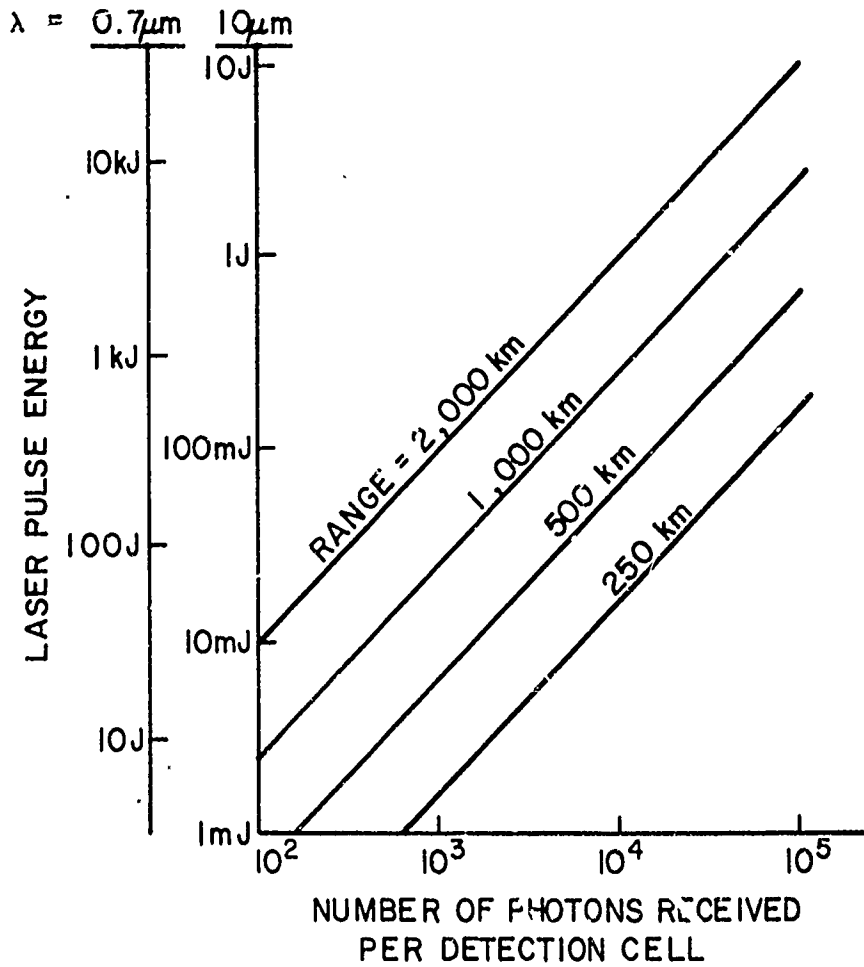


FIG. 7 ENERGY REQUIREMENTS FOR LOW-ALTITUDE LASER CORRELOGRAPHY



$\rho\sigma = 1\text{m}^2$
 $\Omega_i = 10^{-10}\text{srad}$
 10 dB PATH LOSS
 10 m TARGET DIMENSION

74-3-33-0042

RIVERSIDE RESEARCH INSTITUTE

frequency.) For instance, a target at 1,000 km altitude requires 2 mJ from a CO₂ laser and 10 J from a ruby laser, respectively, to return 100 photons per resolution cell. On the basis of this energy comparison, it is concluded that visible lasers are not likely to have adequate energy to provide useful signal-to-noise ratios for target ranges in excess of roughly 1,000 km and that CO₂ lasers are most suitable for the synchronous altitude role.

B. Visible Wavelength System Parameters (See also Paper No. 6.²)

The objectives of a visible wavelength measurements program would be to: 1) evaluate the quality of the correlography and holography; 2) confirm single- and multiple-glint analyses; 3) obtain 10-20 cm data on known and unknown targets; 4) test computation schemes; and 5) combine these data with information obtained from other kinds of sensors.

Table I compares typical current and modified specifications of a ruby laser for making such measurements; note that state-of-the-art pulse energy is adequate, but that both the pulse length and the coherence length must be extended to make them longer than the physical lengths of targets expected to be observed.

Fig. 8 is a schematic diagram of the receiver configuration needed to record the backscatter patterns for computerized analysis of the signatures. The field lens images the intensity distribution in the aperture of the telescope onto a photoelectric image tube; the intensity pattern on the image tube (seen through a band-pass optical filter) is then read into a recording system where off-line data processing is performed to extract target information.

C. Carbon Dioxide System Parameters

Figure 9 shows the transmitter energy needed to obtain various signal-to-noise ratios in each receiver element for target altitudes from 2,000 to 4,000 km; a 1-m receiver aperture is assumed along with 10-dB path loss, 10- μ rad illumination beam-width, and a target reflectivity-area-product equal to 1 m². (These curves follow from the energy considerations presented in the Appendix.) Figure 10 relates to the maximum allowable duration of the laser illumination pulse such that the backscatter pattern moves less than one-half a speckle size during the illumination time. It is seen that for target angle rates of up to 10 mrad/sec, pulse lengths of 50-100 μ sec are adequate for target lengths of up to 10 m transverse dimension.

Because of the large aperture sizes that are needed, the

TABLE I. RUBY LASER SPECIFICATIONS

SPECIFICATION	STATE-OF-THE-ART	MODIFIED
PULSE ENERGY	10 J	10 J
PULSE LENGTH	15 NSEC	≥ 100 NSEC
COHERENCE LENGTH	1-2 cm	10 M

FIG. 8 RECEIVER CONFIGURATION

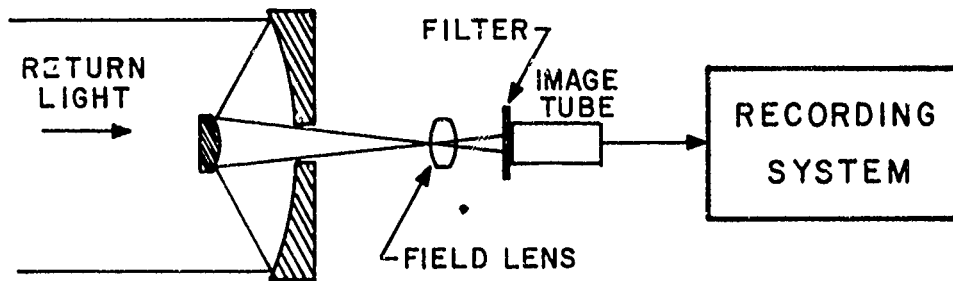
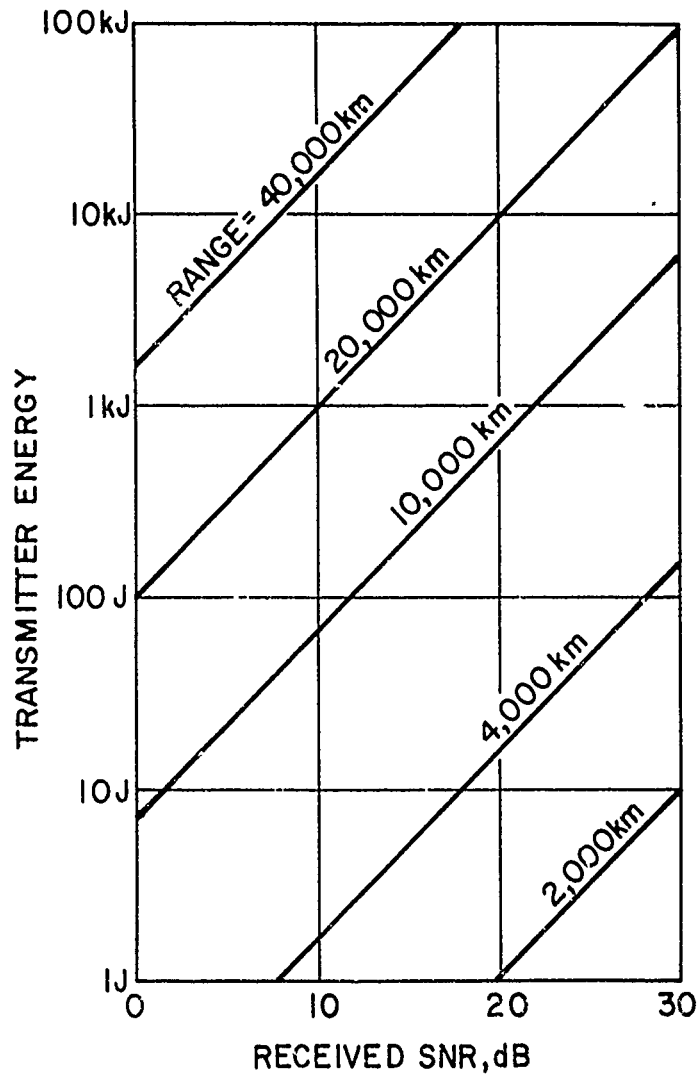


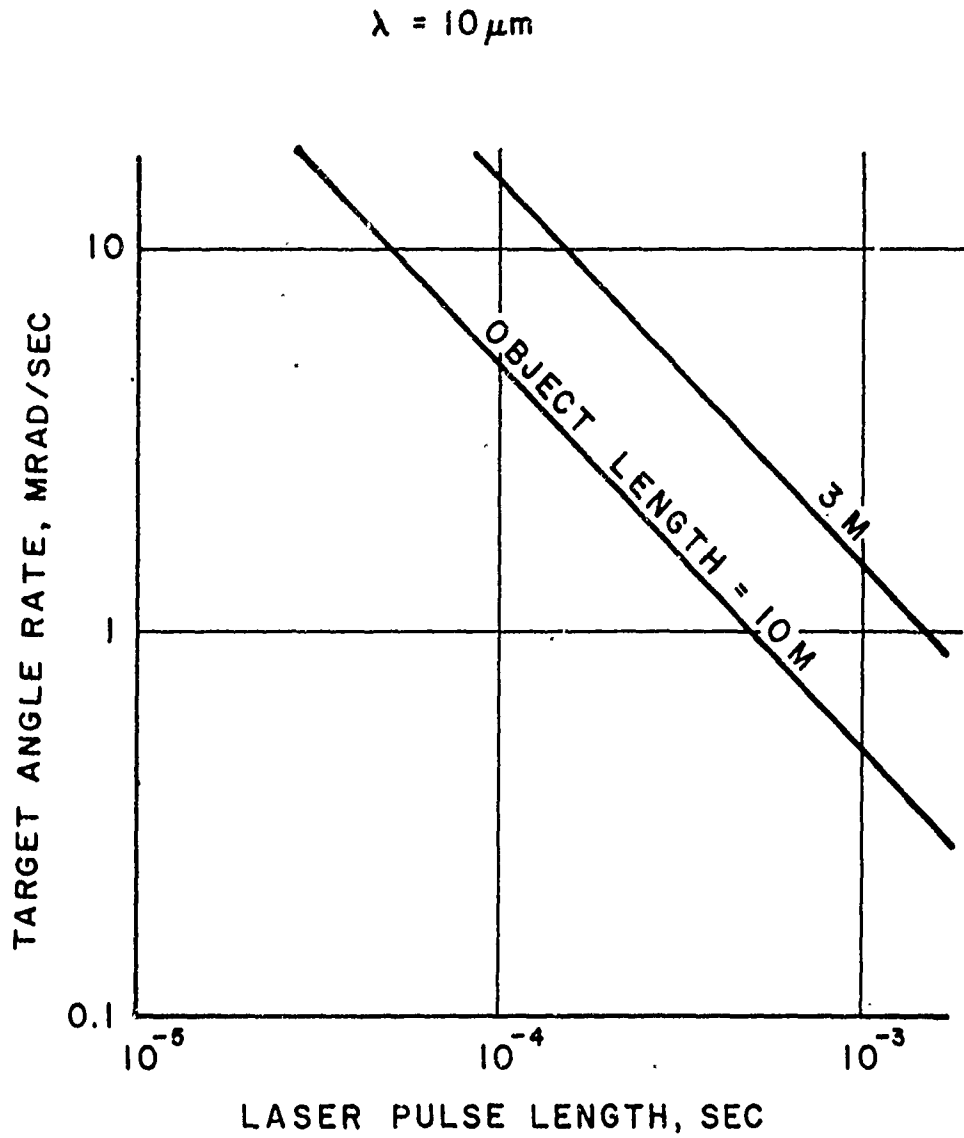
FIG. 9 ENERGY REQUIREMENTS FOR CO₂ LASER



$\lambda = 10 \mu\text{m}$
 $\rho\sigma = 1\text{m}^2$
 $A_{\text{rec}} = 1\text{m}^2$
 10 dB PATH LOSS
 $\Omega_i = 10^{-10} \text{srad}$
 $\eta_q = 0.4$

174-3-33-0040

FIG. 10 MAXIMUM TARGET ANGLE RATE ALLOWABLE FOR
VARIOUS LASER PULSE LENGTHS



RIVERSIDE RESEARCH INSTITUTE

requirement for array receivers (as opposed to contiguous apertures) is self-evident for carbon dioxide systems. The number of elements required in a filled array (an array with a uniform grid of equally spaced telescopes, where the spacing is equal to one-half the minimum expected speckle size) may be related to the number of resolution cells desired on the target.

Fig. 11 is a plot of the required number of array elements as a function of linear resolution on the targets, for maximum target dimensions of 3 and 10 m. It is clear that 10-cm resolution on a 10-m target will require 10,000 elements, and that this is unacceptable. The conclusion is that receiver array thinning is essential; in addition, the thinning must eliminate, for reasons of cost and practicality, over 99% of the elements in order to reduce the numbers to a maximum of 100-200 elements.

A sketch of a receiver subsystem that would be suitable for energy detection in each array element is shown in Fig. 12. Doppler tracking is performed by an electronically tracking local oscillator after an optical heterodyne has been performed on the photo-mixer element. A square-law detector detects the energy in the IF passband and, after low-pass filtering, the signal is recorded. An alternative receiver scheme might make use of a tracking optical local oscillator, although this technology is less adequately developed. This receiver is applicable to on-axis holography and correlography; for off-axis holography, using polarization-sensitive reception, the incoming optical signal would first be passed through a polarizing beam splitter and then be transmitted to two superheterodyne receivers operating in the same way as the one shown up to the IF output. At that point, the output of the two IF amplifiers would be added and passed through a square-law detector; the low-pass filtered output would contain the required interference between the two beams. The polarization-sensitive receiver would require coherent optical and electronic local oscillators in each channel to operate successfully.

FIG. II NUMBER OF ARRAY ELEMENTS FOR EQUAL SPACING

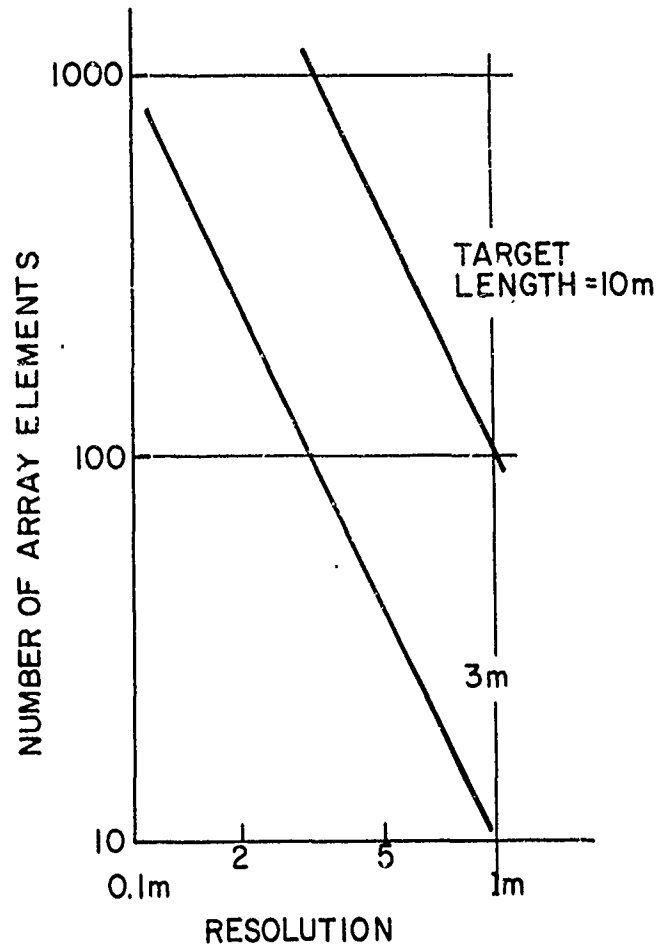
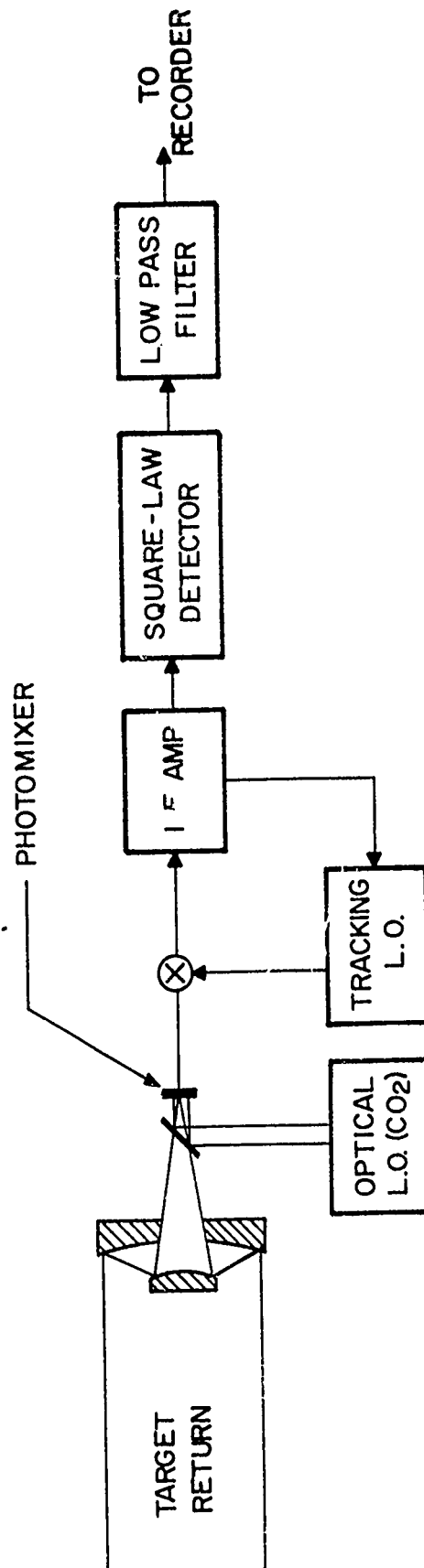


FIG. 12 SUPERHET RECEIVER FOR HOLOGRAMS AND CORRELOGRAMS



74-3-33-0041

RIVERSIDE RESEARCH INSTITUTE

APPENDIX

LASER ILLUMINATOR ENERGY REQUIREMENTS

If a pulsed laser beam of angular width Ω_i , energy W_i and wavelength λ is directed on a target of projected area σ , diffuse reflectivity ρ and range R , then the average number of photons backscattered per unit area in the vicinity of the transmitter is given by

$$n_r = \frac{W_i \lambda \rho \sigma \tau_a}{2\pi hc \Omega_i R^4} \quad (1)$$

where h is Planck's constant, c is the speed of light and τ_a is the round-trip atmospheric transmission factor.

In order to preserve the structure of the backscatter pattern, the aperture area of the receiver* must be smaller than one-half to one-fourth the smallest possible area of a speckle on the ground, the latter quantity being given by λ^2/Ω_t , where Ω_t is the expected maximum solid angle subtended by a target; for 10-m-diameter targets, this limits aperture diameters to less than 1 m for ranges up to about 30,000 km for ruby and 2,000 km for carbon dioxide systems. If it is assumed (somewhat arbitrarily) that maximum aperture diameters for each element of an array receiver will be limited to 1 m by issues of cost and/or practicality then it may be seen that two regimes of photon integration area may be defined; in the low-altitude regime the area over which photons are integrated is limited by speckle size, and in the high-altitude regime this area is limited by receiver element aperture area. In the low-altitude regime, receiver photon integration area is given by

$$A_r = K\lambda^2/\Omega_t = K\lambda^2 R^2/A_t \quad (\text{LOW ALTITUDE}) \quad (2)$$

where A_t is the minimum circular area required to inscribe the maximum target dimension and where $K \sim 1/2$ to $1/4$; for high-altitude,

$$A_r = \text{CONSTANT.} \quad (\text{HIGH ALTITUDE}) \quad (3)$$

*Or, more precisely, the area over which photons may be integrated, and properly called a detection resolution cell.

RIVERSIDE RESEARCH INSTITUTE

The transmitter energy required to produce a given number of photons N_r at the photodetector for receiver area A_r may be computed from Eq. 1 and 2 or 3 for both altitude regimes after noting that the optics transmission factor τ_o may be combined with τ_a to yield a total transmission factor τ . Thus,

$$W_i = \frac{2\pi hc}{K} \frac{\Omega_i A_t R^2 N_r}{\lambda^3 \rho \sigma \tau} \quad (\text{LOW ALTITUDE}) \quad (4)$$

or

$$W_i = 2\pi hc \frac{\Omega_i R^4 N_r}{\lambda \rho \sigma \tau A_r} \quad (\text{HIGH ALTITUDE}) \quad (5)$$

Equations 4 and 5 were used in connection with Figs. 7 and 9, respectively. ($N_r = n_r A_r$.)

RIVERSIDE RESEARCH INSTITUTE

Paper No. 2

INFLUENCE OF THE ATMOSPHERE ON LASER-PRODUCED SPECKLE PATTERNS

(This is an unaltered reproduction of a paper prepared for the 1974 International Optical Computing Conference, April 9-11, 1974, Zürich, Switzerland.⁶ The paper includes a model for laser backscattering, a condensed account of the influence of atmospheric turbulence on the laser correlogram--a fuller account being contained in Paper No. 3--and some qualitative experimental laboratory results. More recent results are contained in a forthcoming Technical Report.¹⁵)

RIVERSIDE RESEARCH INSTITUTE

INFLUENCE OF THE ATMOSPHERE ON LASER PRODUCED SPECKLE PATTERNS*

by

M. King, M. Greenebaum and M. Elbaum
Riverside Research Institute
New York, N.Y. 10023

We analyze the situation of radiation leaving a coherently illuminated rough object and passing through the turbulent atmosphere to a plane of observation where the speckle pattern is measured. Employing a form of the Huygens-Fresnel principle which applies to a spatially inhomogeneous random medium, we find that the effects of the atmospheric turbulence may be represented as a random apodization of the speckle pattern which would be obtained in the non-turbulent case, provided that the entire target lies within a single isoplanatic region. Using experimental data on stellar scintillation to estimate the degree of random apodization for a ground-based receiver observing a near-zenith exo-atmospheric target, we estimate the strength of apodization at selected wavelengths. This analysis shows that one can expect minimal depth of the modulation at 10 μm ; however, patterns formed in the visible region of the spectrum are inclined to suffer substantial apodization. Nevertheless, depending on the scale size of "atmospheric speckles" relative to the range of speckle sizes produced by the target, speckle pattern parameter estimation in the plane of observation may still be possible. This possibility is demonstrated by means of a laboratory simulation experiment. Thus, at least in principle, so long as the normalized autocovariance function of the random apodization is known, both the power spectrum and autocorrelation of the speckle pattern of the object may be determined directly from the statistics of the combined irradiance distribution; these statistics, in turn, yield the correlogram (autocorrelation) and power spectrum of the object.

1. Introduction

It is well known that the speckle pattern generated by a coherently illuminated object carries specific information about the object i.e., the power spectrum of the speckle pattern is equal to the autocorrelation function of the object illumination.^{1,2} In this paper, we evaluate how well this irradiance power spectrum can be estimated when it is subject to degradation by atmospheric turbulence.

First, we shall derive a formula for the power spectrum of the speckle patterns formed from the coherent radiation scattered by an object (two-dimensional, for simplicity), and propagated through the atmosphere. This formula will serve as a basic tool in evaluating the strength and the nature of the atmospheric perturbation. The validity of some of the conclusions derived analytically is demonstrated by experiments described at the end of the paper.

2. Formal Results

A coherently illuminated object is described here by a field distribution $E_0(\vec{p}; t)$. By using the tangent plane approximation, this field can be written as

$$E_0(\vec{p}, t) = r(\vec{p}) I_0^{1/2}(\vec{p}, t) \exp[i k s(\vec{p})], \quad (1)$$

where $I_0(\vec{p}, t)$ is the illumination, r is the reflection coefficient, $s(\vec{p})$ is a random variable describing the surface depth variation about the mean plane, and k is a wave number. For rough objects, it is customary^{1,2} to assume that $s(\vec{p})$ is Gaussian-distributed, with mean zero, and standard deviation σ_s not smaller than the wavelength λ of the radiation used to illuminate the target. As a result of $\sigma_s \geq \lambda$ the autocorrelation function of the object field distribution can be well-approximated by a delta function. Consequently, the fields from different points at the object are independent, and the distribution of this field in space can be regarded as a stochastic process with white noise-like spectrum.

The field at a Fraunhofer observation plane of the object is computed by using³ the extended Huygens-Fresnel principle,

$$E_0(\vec{p}', t) = \sum_{i=1}^N E(\vec{p}_i, t) G(\vec{p}_i, \vec{p}'), \quad (2)$$

where N is the number of independent "cells" into which the field at the object was decomposed, and G is the Green's function

$$G(\vec{p}_i, \vec{p}') = \frac{1}{z} \exp[i k n(\vec{p}_i, \vec{p}') + \psi(\vec{p}_i, \vec{p}')] \quad (3)$$
$$= G_0(\vec{p}_i, \vec{p}') \exp[\psi(\vec{p}_i, \vec{p}')], \quad (3a)$$

where z is the distance between the object plane and the receiver plane; the phase term,

$$\Psi(\vec{p}_i, \vec{p}') = \ell(\vec{p}_i, \vec{p}') + i \phi^a(\vec{p}_i, \vec{p}')$$

is a complex phase perturbation which describes the effects of the inhomogeneous medium, ϕ^a and ℓ representing the phase and the logarithm of the amplitude perturbations, respectively, due to the random inhomogeneities of the atmospheric index,

$$G_0(\vec{p}_i, \vec{p}') = \frac{1}{2} \exp[i k h(\vec{p}_i, \vec{p}')]]$$

is the value of the Green's function in the absence of the turbulent medium, and $h(\vec{p}_i, \vec{p}')$ is the geometric distance between the points \vec{p}_i and \vec{p}' .

The "instantaneous" irradiance of the observation point \vec{p} , $I(\vec{p}')$, is obtained by time-averaging the square of $\text{Re}\{E(\vec{p}', t)\}$ over times small compared with the time it takes for any $\Psi(\vec{p}_i, \vec{p}')$ to change:

$$I(\vec{p}') = \frac{1}{2} \text{Re} \{ E(\vec{p}', t) E^*(\vec{p}', t) \} \quad (5)$$

$$= \frac{1}{2} \text{Re} \left\{ \sum_{i,j} E_0(\vec{p}_i) E_0^*(\vec{p}_j) G_0(\vec{p}_i, \vec{p}') G_0^*(\vec{p}_j, \vec{p}') \exp[\Psi(\vec{p}_i, \vec{p}') + \Psi^*(\vec{p}_j, \vec{p}')] \right\} \quad (5a)$$

$$= \frac{1}{2} \exp 2\ell(\vec{p}_i, \vec{p}') \text{Re} \left\{ \sum_{i,j} E_0(\vec{p}_i) E_0^*(\vec{p}_j) G_0(\vec{p}_i, \vec{p}') G_0^*(\vec{p}_j, \vec{p}') \right\} \quad (5b)$$

where the Eq. (5a) is obtained by inserting Eqs. (3) and (4) into Eq. (5), and Eq. (5b) results from the assumption that the object lies well within the isoplanatic region, i.e., that $\Psi(\vec{p}_i, \vec{p}') = \Psi(\vec{p}_j, \vec{p}')$ with $i \neq j$ and $i, j = 1, 2, \dots, N$. Beginning with Eq. (5a), the time-dependence of the fields is suppressed to simplify the notation.

In the absence of the random medium, $\Psi = 0$, $I(\vec{p}')$ reduces to $I_0(\vec{p}')$, the object speckle pattern:

$$I_0(\vec{p}') = \frac{1}{2} \text{Re} \{ E_s(\vec{p}') E_s^*(\vec{p}') \} \quad (6)$$

where $E_s(\vec{p}') = \sum_{i=1}^N E_0(\vec{p}_i) G_0(\vec{p}_i, \vec{p}')$.

$\bar{I}(\vec{p}')$, the expected value of $I_0(\vec{p}')$, in the sense of an ensemble average over many realizations of the surface roughness, can be shown to be equal to

$$\bar{I}(\vec{p}') = \frac{1}{2z^2} \sum_{i=1}^N I_0(\vec{p}_i) \quad (7)$$

The term, $I_0(\vec{p}')$, is referred to as the atmospheric speckle noise. It is the irradiance distribution which would be present at the receiver point \vec{p}' when a coherent point source of strength $\bar{I}(\vec{p}')$ is present at some object point \vec{p}_0 :

$$I_A(\vec{p}') = \bar{I}(\vec{p}') \exp[2\ell(\vec{p}', \vec{p}_0)] \quad (8)$$

It has been shown⁴ that the expected value of I_A taken as an ensemble average over many realizations of the atmospheric turbulence is equal $\bar{I}(\vec{p}')$. Using Eqs. (8) and (9), we rewrite the expression for the instantaneous irradiance distribution $I(\vec{p}')$, in terms of the expected value of $I(\vec{p}')$, $\bar{I}(\vec{p}')$, randomly modulated by both the object

and the atmospheric speckles, i.e.,

$$I(\vec{p}') = \bar{I}(\vec{p}') \left[1 + \frac{I_A(\vec{p}') - \bar{I}(\vec{p}')}{\bar{I}(\vec{p}')} \right] \left[1 + \frac{I_0(\vec{p}') - \bar{I}(\vec{p}')}{\bar{I}(\vec{p}')} \right] \quad (9)$$

It is easy to see that the normalized autocovariance function of $I(\vec{p}')$, $C(\vec{p}', \vec{p}' + \Delta\vec{p}')$, can be written as a sum of three terms: a target-related term which is the normalized autocovariance function of $I_0(\vec{p}')$, an atmosphere turbulence-related term, which is the normalized autocovariance function of $I_A(\vec{p}')$, and their product.

$$C(\vec{p}', \vec{p}' + \Delta\vec{p}') = \frac{\overline{[I(\vec{p}') - \bar{I}][I(\vec{p}' + \Delta\vec{p}') - \bar{I}]}}{\bar{I}^2} = C_A + C_0 + C_A C_0 \quad (10)$$

$$\text{where: } C_A = \frac{\overline{[I_A(\vec{p}') - \bar{I}_A][I_A(\vec{p}' + \Delta\vec{p}') - \bar{I}_A]}}{\bar{I}_A^2}$$

$$C_0 = \frac{\overline{[I_0(\vec{p}') - \bar{I}_0][I_0(\vec{p}' + \Delta\vec{p}') - \bar{I}_0]}}{\bar{I}_0^2}$$

and $\bar{I}(\vec{p}') = \bar{I}(\vec{p}' + \Delta\vec{p}') = \bar{I}$ has been assumed.

The spectrum of $I(\vec{p}')$, S , is computed by taking the Fourier transform of the normalized covariance function (10)

$$S = S_A + S_0 + S_A * S_0 \quad (11)$$

where S_A and S_0 are the Fourier transforms of C_A and C_0 respectively, and $*$ denotes the convolution operation.

3. Discussion of Formal Results

We want to know how well the spectrum S of the speckle pattern randomly modulated by the atmospheric noise approximates the object-related power spectrum, S_0 .

Several conclusions can be drawn from a slightly modified form of Eq. (10):

$$C = C_0 + C_A (C_0 + 1) \quad (10a)$$

We observe first that the function C approximates the function of interest, C_0 , if at least one of the following conditions is satisfied:

(a) $C_A \ll C_0 \leq 1$ for all values of the lag, $\Delta\vec{p}'$.

(b) $L_A \ll L$ where L_A and L are measures of the width of the correlation functions $\overline{[I_A(\vec{p}') - \bar{I}_A][I_A(\vec{p}' + \Delta\vec{p}') - \bar{I}_A]}$ and $\overline{[I_0(\vec{p}') - \bar{I}_0][I_0(\vec{p}' + \Delta\vec{p}') - \bar{I}_0]}$ respectively.

The inequality (a) requires, in particular, that the normalized standard deviation of turbulence generated "atmospheric speckle noise", $C_A(\vec{p}', \vec{p}') = \sigma_A^2 / \bar{I}_A^2$ be much smaller than the normalized standard deviation of the object related "signal", $C_0(\vec{p}', \vec{p}') = \sigma_0^2 / \bar{I}_0^2 = 1$. Inequality (a) therefore signifies that the depth of modulation of the atmospheric speckles considered as a "noise" is much smaller than that of the "signal".

On the other hand, inequality (b) is satisfied when the half-width, L_A , of the correlation function of the "noise", $\langle I_A(\vec{p}') I_A(\vec{p}' + \Delta\vec{p}') \rangle$, is much smaller than the half-width, L_O , of the correlation function of the "signal", $\langle I_O(\vec{p}') I_O(\vec{p}' + \Delta\vec{p}') \rangle$. As one can see from Eq. (10a) the function $C(\vec{p}', \vec{p}' + \Delta\vec{p}')$ closely approximates $C_O(\vec{p}', \vec{p}' + \Delta\vec{p}')$ for all values of the lag $\Delta\vec{p}'$ larger than L_A when (b) is satisfied. In the "noise"-related second term of Eq. (10a), C_A imposes a "lag window" on the "signal"-related term C_O . The narrower the correlation function C_A with respect to the correlation C_O , the wider the spectrum of "noise" S_A will be with respect to the spectrum of "signal" S_O . If the favorable situation of condition (b) exists, one may scan the noisy irradiance distribution with an aperture small enough to resolve the speckle-pattern "signal" and sufficiently large to average out the turbulence-generated "noise", (i.e., integrate over the structure of characteristic size L_A).

We may now turn to the available experimental data in order to find out under what conditions the atmosphere is sufficiently cooperative for (a) to hold. It is known from stellar scintillation data that, for vertical propagation in the visible spectrum, the normalized variance of the turbulence-related term $\sigma_{I_A}^2/I^2$ is approximately ~ 0.2 .⁵ The situation at 10.6μ , at least for vertical paths at night and scaling the visible scintillation according to the $\lambda^{-7/6}$ law,⁴⁻⁶ is expected to be even more encouraging, i.e., $\sigma_{I_A}^2/I^2 \sim 0.008$. However, for near-horizontal propagation under "saturation-of-scintillation" conditions, e.g., propagation over paths in excess of ~ 1 km in the visible or ~ 10 km at 10.6μ , $\sigma_{I_A}^2/I^2 \sim 10$ and the condition (a) is not L_A satisfied.⁴⁻⁶

As to the second condition, (b), we note that the width, L_O , of the autocorrelation function of the "signal" is proportional to $\lambda z/D$, where D is the "aperture size" of the object, e.g., the diameter of a uniformly reflecting, uniformly illuminated object. On the other hand, the "noise" correlation length, L_A , is approximately $(\lambda L)^{1/2}$, where L is on the order of the path length through uniform turbulence (e.g., horizontal propagation) or the height to the tropopause for vertical propagation.^{5,6} Based on measurements of "shadow bands" in stellar astronomy, $(\lambda L)^{1/2}$ can be expected to vary from 3 or 4 to 7 or 8 cm in the visible.⁶

* The third condition, $L_O \ll L_A$, is likely to be of practical importance unless condition (a) is also satisfied. For details, see Ref. 4.

Condition (b), which requires that $(\lambda L)^{1/2} < \lambda z/D$, is satisfied for objects with transverse dimensions of meters, at ranges 10 km or greater in the visible.

In summary, the theoretical prediction supported by experimental data shows that there are situations where it will be possible to obtain reliable information about the object from the power spectrum of the object speckle pattern randomly apodized by the atmosphere. These situations, given above as conditions (a) and (b), are more easily satisfied in the infrared than in the visible spectrum.

4. Experimental Results

To simulate a diffusely reflecting object, an apertured ground-glass diffuser was used to phase-modulate a collimated laser beam ($\lambda = 0.5 \mu$) in transmission. A silicon-diode array vidicon (effective aperture $0.13 \text{ mm} \times 0.01 \text{ mm}$) located 1.8 m from the object, was capable of resolving the minimum speckle size in the speckle pattern scattered by the object. Directly in front of the diode array ($\approx 3 \text{ mm}$ away) was placed a photographic transparency containing a simulated "atmospheric speckle pattern". (This transparency was made by recording the speckle pattern produced by a $2 \times \frac{1}{2} \text{ mm}^2$ diffuse target at a distance of 1.8 meters. After 4 min of development in DK-50 at 68° F the mean amplitude transmission of the Ektapan recording film was approximately 50%. Consequently the irradiance fluctuations cause a severe amplitude modulation to be recorded which subsequently appears on the field passing through the transparency. The film backing and the emulsion thickness variations tend to produce some phase modulation which must be taken into account in the detailed interpretation.)

The output of the vidicon provides an analog spectrum analyzer with an irradiance distribution (e.g., Fig. 1 (b)) which is used to obtain the power spectrum of the sample. Individual power spectrum estimates were obtained by sampling in one direction at 0.01-mm intervals over 7.5 mm of the speckle pattern and averaging over 0.13 mm in the orthogonal direction.

To obtain a sufficient number of random samples, in order to estimate the power spectrum to an empirically sufficient degree of accuracy, 31 different realizations of the object phase structure were generated by exposing non-overlapping areas of the ground glass to the collimated beam. The arithmetic mean of these individual spectral realizations (displayed as S_O and S_O' , respectively in Figs. (1) and (2)) estimates the power spectrum of the object speckle pattern. This can be compared with the estimator of the power spectrum (S and S' in Figs. (4) and (5), respectively) of the object speckle pattern randomly apodized by the photographic transparency. (The spectra in Figs. (4) and (5) are obtained as an arithmetic mean of 31 individual spectrum estimates, each obtained for a particular realization of the object phase structure and of the film transparency perturbation.)

RIVERSIDE RESEARCH INSTITUTE

Of the two objects, one (Fig. 1 (a)) had a wider spectrum, and the other (Fig. 2 (a)) a narrower spectrum, than that of the simulated atmosphere (Fig. 3). Upon comparing the spectra displayed in Figs. 1 and 4 and those in Figs. 2 and 5, we observe that the general features of the spectra are preserved in the presence of the perturbation i.e., neither size nor shape is seriously affected.

The authors wish to thank L. Schlom and P. Wong for carrying out the experiments.

This work was supported by ARPA.

References

1. J.W. Goodman, "Statistical Properties of Laser Sparkle Patterns," Tech. Rept. SEL-63-140 (TR 2303-1), Stanford Univ. Electronics Lab, Stanford, Cal., Dec. 1963; Proc. I.E.E.E. 53, 1688 (1965).
2. L.I. Goldfischer, J.Opt. Soc. Amer., 55, 247 (1965).
3. R.F. Lutomirski and H.T. Yura, Appl. Optics 10, 1652 (1971).
4. M. Greenebaum and M. King, "Laser-Produced Speckle Patterns as Seen through a Randomly Inhomogeneous Atmosphere," (to be published).
5. V.I. Tatarskii, The Effects of Turbulent Atmosphere on Wave Propagation, Israel Program for Scientific Translations, Jerusalem, 1971. (Available from National Technical Information Service, Springfield, Va. 22151.)
6. R.S. Lawrence and J. W. Strohbehn, Proc. I.E.E.E. 58, 1523 (1970).

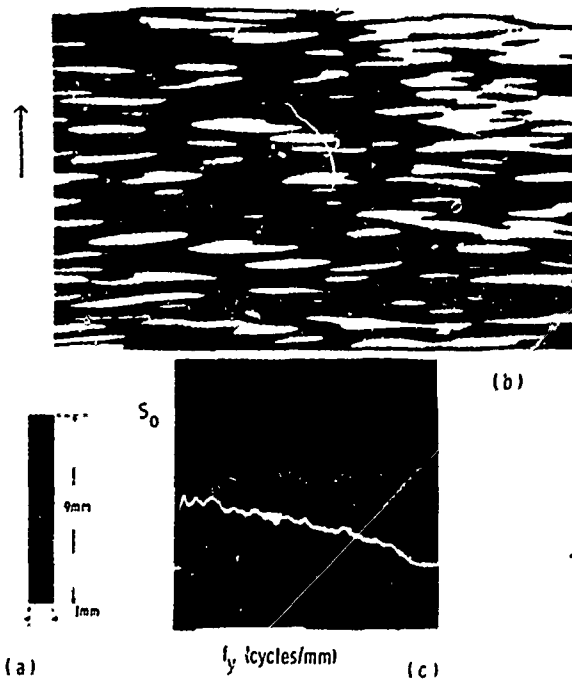


Fig. 1: (a) Object. (b) Speckle pattern of object. (c) S_0 , Spectrum of (b), vs. spatial frequency, f_y .

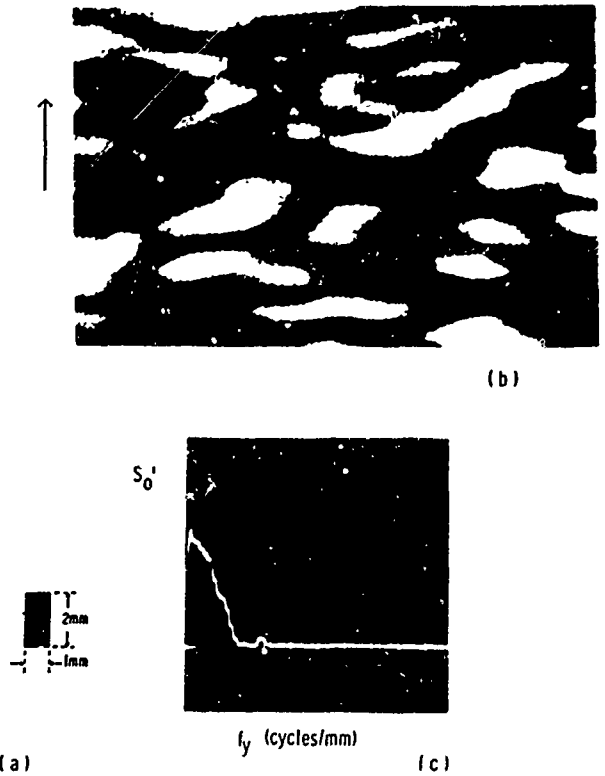


Fig. 2: (a) Object. (b) Speckle pattern of object. (c) S'_0 , Spectrum of (b), vs. spatial frequency, f_y .

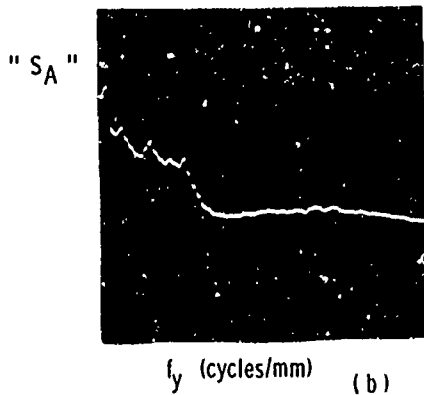
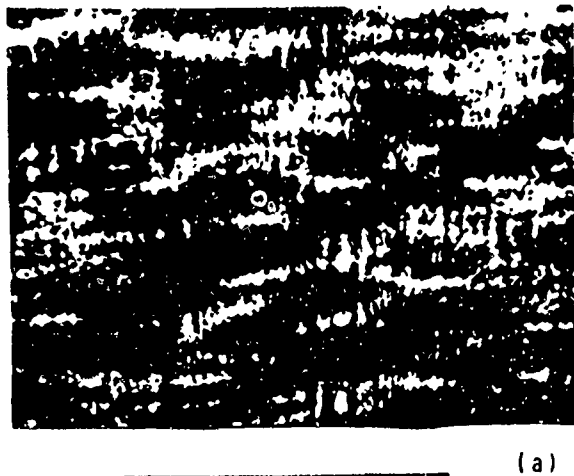


Fig. 3: (a) "Atmospheric" speckle pattern. (b) " S_A ", Spectrum of (a) vs. spatial frequency, f_y .

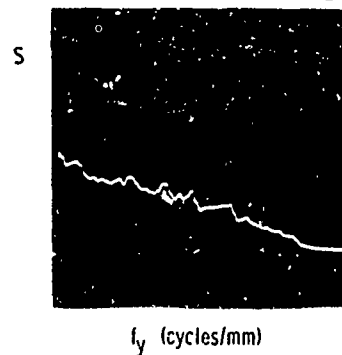


Fig. 4: Spectrum of speckles from object in Fig. 1(a) as modulated by "atmospheric" speckles in Fig.3(a).

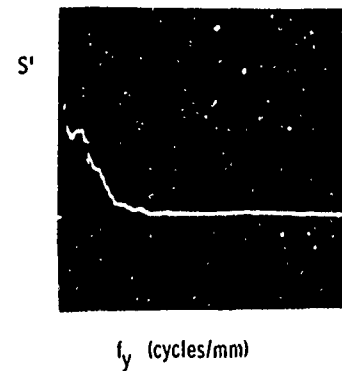


Fig. 5: Spectrum of speckles from object in Fig. 2(a) as modulated by "atmospheric" speckles in Fig.3(a).

RIVERSIDE RESEARCH INSTITUTE

Paper No. 3

LASER-PRODUCED SPECKLE PATTERNS AS SEEN THROUGH A RANDOMLY INHOMOGENEOUS ATMOSPHERE

(The following is a reproduction of the latest revision of RRI Technical Paper PTP-100(R), 21 December 1973. Previous versions of this paper appeared under the same title as Technical Paper PTP-100, 25 June 1973, and as Research Note N-8/174-3-33, 28 November 1972.⁴)

This paper is a first-principles account of the reason why laser correlography is insensitive to atmospheric phase fluctuations, and includes some estimates of the residual effects of turbulence (related to scintillation). A ground-based receiver, an exoatmospheric space object with a rough surface, isoplanatism, and an idealized (space-based) laser illuminator are assumed. See Paper No. 4 for the effect of relaxing some of these constraints.

RIVERSIDE RESEARCH INSTITUTE

LASER-PRODUCED SPECKLE PATTERNS AS SEEN THROUGH A RANDOMLY INHOMOGENEOUS ATMOSPHERE

Michael Greenebaum and Marvin King

Riverside Research Institute, 80 West End Ave., New York, N. Y. 10023

The spatial autocovariance function of the irradiance distribution received in the backscatter direction from a target illuminated uniformly by a laser is considered in the presence of an intervening turbulent atmosphere. When the target is perfectly diffuse and lies entirely within a single isoplanatic region of the receiver aperture, the effect of the atmospheric turbulence is to produce a random apodization of the irradiance distribution. From this randomly apodized irradiance distribution, one may recover the autocovariance function which would be obtained in the absence of turbulence. This non-turbulent autocovariance function is proportional to the far-field diffraction pattern corresponding to the object illumination function, while the associated power spectral density is proportional to the target "correlogram".

RIVERSIDE RESEARCH INSTITUTE

Introduction

It is well known that the backscattered irradiance from a rough, laser-illuminated target has a speckled appearance.¹⁻⁴ The second-order statistics of this irradiance distribution convey spatial information concerning the target in a manner similar to the van Cittert-Zernike theorem: the spatial autocovariance function of the random irradiance pattern is proportional to the far-field diffraction pattern corresponding to the object illumination function; the associated power spectral density is proportional to the "correlogram" of the object illumination function.²⁻⁴ In the present paper, we examine the autocovariance and power spectral density of the irradiance for the case where a turbulent atmosphere intervenes between the target and the entrance pupil of the receiving telescope.

To keep the underlying interference phenomena in the forefront, we base our analysis on the random-phase, identical-strength, point-scatterer target model and calculational approach of Goldfisher.³ Using a form of the Huygens-Fresnel principle which applies to a spatially inhomogeneous random medium,⁵⁻⁶ we extend this analysis to the case where the radiation leaving a coherently illuminated target passes through the turbulent atmosphere. Provided that the entire target lies within a single isoplanatic region, the effect of the atmospheric turbulence is shown to reduce to a random apodization of the irradiance distribution which would be obtained in the non-

RIVERSIDE RESEARCH INSTITUTE

turbulent case. The autocovariance function is represented therefore as the sum of a target-related speckle term, a term arising from the random apodization by the turbulence, and their product (Eq. (20)).

When experimental data on stellar scintillation are used to estimate the degree of random apodization to be expected, we conclude that the turbulence effect is small in favorable cases, e. g., a ground-based receiver observing a near-zenith exoatmospheric target illuminated at $10.6 \mu\text{m}$. Then the second-order statistics retain their "van Cittert-Zernike theorem-like" significance. In general, it is possible to extract the desired target-related second-order statistics from the randomly apodized irradiance distribution, regardless of the strength of the apodization, so long as the normalized autocovariance function of the apodization is known from auxiliary data (e. g., on appropriately filtered starlight).

Although the details are not carried out explicitly here, the methods used in this paper are capable of fairly straightforward generalization to estimate the effects of violating the isoplanatic patch condition.

The coordinate system shown in Fig. 1 is used throughout. Points \vec{p}' on the coherently illuminated target have coordinates $(u, v, 0)$. The radiation scattered from the (exoatmospheric) target passes through the turbulent atmosphere to the (ground-based) telescope receiver aperture located at a distance h . The

irradiance at each point \vec{p} in the entrance aperture is recorded. The points \vec{p} have coordinates (x,y,h) . For simplicity, a planar target is assumed, and the plane of the receiver aperture is taken as parallel to the plane of the target.

The Generalized Huygens-Fresnel Principle

For propagation distances large compared with the size of a radiating aperture, it has been shown^{5, 6} that the Huygens-Fresnel principle may be extended to the spatially inhomogeneous random medium. According to this principle, the field due to an arbitrary complex disturbance over the radiating aperture can be computed by superposition of the fields due to spherical wavelets leaving each aperture element. The propagation of an arbitrary wavefront is then determined by the way a spherical wave propagates through an instantaneous realization of the inhomogeneous random medium. The complex field at the observation point \vec{p} due to a point source at \vec{p}' in the plane of the transmitting aperture (which is identical to the field at \vec{p}' due to a point source at \vec{p}) is given by:

$$G(\vec{p}', \vec{p}) = G(\vec{p}, \vec{p}') = s^{-1} \exp [iks + \psi(\vec{p}, \vec{p}')] , \quad (1)$$

where $s = |\vec{p} - \vec{p}'|$ is the geometric distance between the field point \vec{p} and the source point \vec{p}' ,

$k = 2\pi/\lambda =$ optical wavenumber, and

$\psi(\vec{p}, \vec{p}') = \ell(\vec{p}, \vec{p}') + i \phi^a(\vec{p}, \vec{p}')$ describes the effects of the inhomogeneous medium upon the propagation of a spherical wave.⁶

$\text{Re } \psi = \ell$ represents the logarithm of the amplitude perturbation due to the random inhomogeneities of the atmospheric refractive index, and $\text{Im } \psi = \phi^a$ represents the phase perturbation arising from the same inhomogeneities.

Calculation of Backscattered Irradiance

As the first step in our calculation of the second-order statistics of the irradiance distribution, we consider the complex field scattered from the target when the propagation takes place in a non-turbulent medium. The target is modelled as a collection of diffuse scatterers, each occupying an area $\Delta u \Delta v \ll \lambda^2$ over which the reflected irradiance $P(u, v) = P(u, v, 0)$ may be considered constant.⁷ Each scatterer contributes a field at the observation point \vec{p} at time t , which is dependent upon the reflected irradiance $P(u, v)$ leaving the target at the point $\vec{p}' = (u, v, 0)$ at the time $t' = t - s/c$, and upon $\phi^S(u, v)$, a random phase angle associated with the scatterer at \vec{p}' .

Now we let a spatially inhomogeneous medium intervene between \vec{p}' and \vec{p} . By means of the extended Huygens-Fresnel principle, Eq. (1), we may obtain the field contribution at time t at point $\vec{p} = (x, y, h)$ due to the same scatterer after the wave has propagated through the turbulent atmosphere, i. e.,

$$\left[\tau P(u, v) \Delta u \Delta v / \pi s^2 \right]^{1/2} \text{Re exp} [ik(ct - s) + i \phi^t(u, v)] \dots(2)$$

where c = speed of light in the medium,

$$\phi^t(u, v) = \phi^S(u, v) - i\psi(\vec{p}, \vec{p}') = \phi^S(u, v) - i\psi(u, v, 0; x, y, h),$$

τ = atmospheric transmission between $(u, v, 0)$ and (x, y, h) ,

$P(u, v)$ = reflected irradiance (or "object illumination function")³, the product of the irradiance incident upon the target surface and $\rho_d(u, v)$, the (hemispherical) diffuse reflectance at (u, v) . $P(u, v)$ is the "scene".

RIVERSIDE RESEARCH INSTITUTE

The correlation between the real random variables, $\phi^S(u,v)$, and the complex random variable, $\psi(u,v,0;x,y,h)$, is identically zero, since these quantities are associated with physically distinct and independent processes. As discussed in Appendices A and B, $\phi^S(u,v)$ is assumed to be Gaussian-distributed, with zero mean and standard deviation greater than π ,^{8,9} whereas $\psi(u,v,0;x,y,h)$ is assumed to be a complex Gaussian process with effectively uncorrelated real and imaginary parts, an assumption which is well-founded experimentally.¹⁰

In the Fresnel approximation, the contribution of the scatterer at $(u,v,0)$ to the field at (x,y,h) is given by:

$$\begin{aligned} & [\tau P(u,v) \Delta u \Delta v / \pi h^2]^{1/2} \exp [i \ell(u,v;x,y)] \\ & \cdot \cos \left[\frac{2\pi}{\lambda} (ct + \frac{xu+yv}{h}) + \theta(x,y) + \phi'^S(u,v) + \phi^a(u,v;x,y) \right], \end{aligned} \quad \dots(3)$$

where $\theta(x,y) = - \frac{2\pi}{\lambda} (h + \frac{x^2+y^2}{2h})$, and

$$\phi'^S(u,v) = \phi^S(u,v) + \frac{\pi}{\lambda h} (u^2 + v^2) .$$

The weak trend in the phase, $\phi'^S(u,v)$, produced by the quadratic Fresnel term associated with the scatterer at $(u,v,0)$ may be absorbed without significantly affecting the randomness.³ Thus, $\phi'^S(u,v)$ is also a Gaussian-distributed random phase with large variance.⁸ The z-dependence of $\phi^a(u,v;x,y)$ is suppressed in the notation; ϕ^a gives explicitly the phase perturbation introduced by the atmospheric inhomogeneities which are present along a particular path, from $(u,v,0)$

RIVERSIDE RESEARCH INSTITUTE

to (x, y, h) . Similar comments hold for the notation given the log-amplitude perturbations, $\ell(u, v; x, y)$.

$E(x, y) = E(x, y, h)$, the total field at (x, y, h) in the receiver aperture (Fig. 1), is obtained by superimposing the contributions from all scatterers in the $(u, v, 0)$ plane:

$$\begin{aligned}
 E(x, y) = & \left[\frac{T \Delta u \Delta v}{\pi h^2} \right]^{1/2} \left\{ \cos \left(\frac{2\pi}{\lambda} ct + \theta(x, y) \right) \sum_{u, v} [P(u, v)]^{1/2} \right. \\
 & \cdot \exp [\ell(u, v; x, y)] \cos \left[\frac{2\pi}{\lambda} \left(\frac{xu + yv}{h} \right) + \phi^s(u, v) + \phi^a(u, v; x, y) \right] \\
 & \quad \left. - \sin \left(\frac{2\pi}{\lambda} ct + \theta(x, y) \right) \sum_{u, v} [P(u, v)]^{1/2} \right. \\
 & \cdot \exp [\ell(u, v; x, y)] \sin \left[\frac{2\pi}{\lambda} \left(\frac{xu + yv}{h} \right) + \phi^s(u, v) + \phi^a(u, v; x, y) \right] \left. \right\} . \\
 & \dots(4)
 \end{aligned}$$

We now average the square of $E(x, y)$ over times long compared with the period of the optical radiation, but short compared with the time it takes for $\phi^a(u, v; x, y)$, $\ell(u, v; x, y)$, or $\phi^s(u, v)$ to change. The result is the "instantaneous" irradiance at (x, y, h) :

$$\begin{aligned}
 H(x, y) = & \frac{T \Delta u \Delta v}{2\pi h^2} \left\{ \left(\sum_{u, v} [P(u, v)]^{1/2} \exp [\ell(u, v; x, y)] \right. \right. \\
 & \quad \left. \cdot \cos \left[\frac{2\pi}{\lambda} \left(\frac{xu + yv}{h} \right) + \phi^s(u, v) + \phi^a(u, v; x, y) \right] \right)^2 \\
 & \quad + \left(\sum_{u, v} [P(u, v)]^{1/2} \exp [\ell(u, v; x, y)] \right. \\
 & \quad \left. \cdot \sin \left[\frac{2\pi}{\lambda} \left(\frac{xu + yv}{h} \right) + \phi^s(u, v) + \phi^a(u, v; x, y) \right] \right)^2 \left. \right\} \\
 & \dots(5)
 \end{aligned}$$

The sum of the squares of each term in the series is independent of the phase angles of the individual scatterers, as

well as of the turbulence-related phase angles. This sum, which is given by

$$\bar{H}(x,y) = \frac{\tau \Delta u \Delta v}{2\pi h^2} \sum_{u,v} P(u,v) \exp [2\ell(u,v;x,y)]$$

$$\xrightarrow[\Delta v \rightarrow 0]{\Delta u \rightarrow 0} \frac{\tau}{2\pi h^2} \int_{-\infty}^{\infty} du \int_{-\infty}^{\infty} dv P(u,v) \exp [2\ell(u,v;x,y)], \quad \dots(6)$$

is the irradiance distribution which would be obtained under noncoherent illumination of the target, for a single realization of the random apodization produced by the atmosphere. In other words, Eq. (6) may be considered to result from an average over an ensemble of random target phases, $\phi^S(u,v)$, for a single realization of the turbulence.

The terms remaining in the series expansion of Eq. (5) after Eq. (6) is subtracted will be denoted by the symbol, $\tilde{H}(x,y)$, i. e., $\tilde{H}(x,y) = H(x,y) - \bar{H}(x,y)$. In the case of a uniformly illuminated target and no turbulence in the intervening medium, $\tilde{H}(x,y)$ represents the variation of the speckle pattern about the mean over the plane of observation.³ More generally, in the presence of turbulence, we interpret $\tilde{H}(x,y)$ as the difference between the irradiance measured at the plane of the receiver aperture when the target is coherently illuminated and the irradiance which would be measured upon scattering from a similar noncoherently illuminated target. (The same instantaneous realization of the turbulent atmosphere and of the rough surface is presumed under both illumination conditions.) Expanding Eq. (5) and deleting all terms contributing to $\bar{H}(x,y)$, we obtain:

RIVERSIDE RESEARCH INSTITUTE

$$\begin{aligned} \bar{H}(x,y) = & \frac{\tau \Delta u \Delta v}{2\pi h^2} \sum_{u,v} \sum_{\omega,\Omega} \left[P(u,v) P\left(u - \frac{\lambda h \omega}{2\pi}, v - \frac{\lambda h \Omega}{2\pi}\right) \right]^{1/2} \\ & \cdot \exp \left[\iota(u,v;x,y) + \iota\left(u - \frac{\lambda h \omega}{2\pi}, v - \frac{\lambda h \Omega}{2\pi}; x,y\right) \right] \\ & \cdot \left[\cos \left[\omega x + \Omega y + \Psi(\omega,\Omega;u,v;x,y) \right] - \delta_{\omega 0} \delta_{\Omega 0} \right], \end{aligned} \quad (7)$$

where $u' = u - \frac{\lambda h \omega}{2\pi}$, $v' = v - \frac{\lambda h \Omega}{2\pi}$, i. e.,

$$\omega = \frac{2\pi}{\lambda h}(u - u'), \quad \Omega = \frac{2\pi}{\lambda h}(v - v'),$$

$$\begin{aligned} \Psi(\omega,\Omega;u,v;x,y) = & \rho^{iS}(u,v) - \rho^{iS}\left(u - \frac{\lambda h \omega}{2\pi}, v - \frac{\lambda h \Omega}{2\pi}\right) \\ & + \rho^a(u,v;x,y) - \rho^a\left(u - \frac{\lambda h \omega}{2\pi}, v - \frac{\lambda h \Omega}{2\pi}; x,y\right), \quad \text{and} \end{aligned}$$

$$\delta_{ab} = \begin{cases} 1 & \text{when } a = b, \\ 0 & \text{when } a \neq b. \end{cases}$$

The notation used is similar to that of Ref. 3; $\omega/2\pi$ and $\Omega/2\pi$ are spatial frequencies in the x- and y-directions, respectively. The Kronecker deltas remove the terms for which $\omega = \Omega = 0$, ones that contribute to $\bar{H}(x,y)$. Any single term in Eq. (7) describes the interference fringe generated in the plane of observation by a pair of point scatterers on the diffuse surface, one at the point $(u,v,0)$ and the other at the point $(u - \frac{\lambda h \omega}{2\pi}, v - \frac{\lambda h \Omega}{2\pi}, 0)$, as seen through the intervening randomly inhomogeneous atmosphere. $\Psi(\omega,\Omega;u,v;x,y)$ is a random phase angle, so that one has a superposition of a random collection of high-contrast interference fringes, so long as the observation time is short compared with the time it takes for $\iota(u,v;x,y)$ and $\rho^a(u,v;x,y)$ to change appreciably.¹¹ Moreover, it is clear from the definition

that $\Psi(0,0;u,v;x,y) \equiv 0$, for any point (u,v) on the target surface and any point (x,y) in the telescope entrance aperture.

Letting angular brackets denote the ensemble mean, i. e., the average over all possible realizations of the random variables, ℓ , ϕ^a , and ϕ^s , we show in Appendix A that

$$\langle \tilde{H}(x,y) \rangle = 0. \quad (8)$$

It follows that the ensemble mean irradiance,

$$\begin{aligned} \langle H(x,y) \rangle &= \langle \bar{H}(x,y) \rangle \\ &= \frac{\tau}{2\pi h^2} \int_{-\infty}^{\infty} du \int_{-\infty}^{\infty} dv P(u,v) \langle \exp 2\ell(u,v;x,y) \rangle \\ &= \frac{\tau}{2\pi h^2} \int_{-\infty}^{\infty} du \int_{-\infty}^{\infty} dv P(u,v) = \bar{H}_0, \end{aligned} \quad (9)$$

the mean value of the irradiance in the absence of turbulence, since conservation of energy¹² requires

$$\langle \exp 2\ell(u,v;x,y) \rangle = 1. \quad (10)$$

RIVERSIDE RESEARCH INSTITUTE

Spatial Autocovariance of the Irradiance

From the expressions for the irradiance $H(x,y)$, Eqs. (6) and (7), we can obtain directly the spatial autocorrelation function, $\langle H(x,y) H(x+\xi, y+\zeta) \rangle$, i. e., the ensemble average of the product of the irradiances at pairs of points in the receiver aperture. If we assume that the random variable l is effectively uncorrelated with the random variables, ρ^a and ρ^s , (in the sense required in Appendix A), then in the notation³

$$\Delta\omega = \frac{2\pi}{\lambda h} \Delta u ; \quad \Delta\Omega = \frac{2\pi}{\lambda h} \Delta v , \quad (11)$$

the autocorrelation of the total irradiance distribution¹³ becomes:

$$\begin{aligned} \langle H(x,y) H(x+\xi, y+\zeta) \rangle &= \frac{\tau^2 \lambda^2}{16\pi^4 h^2} \sum_{u,v} \sum_{u',v'} [P(u,v) P(u',v')]^{1/2} \Delta u \Delta v \\ &\cdot \sum_{\omega, \Omega} \sum_{\omega', \Omega'} [P(u - \frac{\lambda h \omega}{2\pi}, v - \frac{\lambda h \Omega}{2\pi}) P(u' - \frac{\lambda h \omega'}{2\pi}, v' - \frac{\lambda h \Omega'}{2\pi})]^{1/2} \Delta\omega \Delta\Omega \\ &\cdot \langle \exp [l(u,v;x,y) + l(u',v';x+\xi, y+\zeta) \\ &\quad + l(u - \frac{\lambda h \omega}{2\pi}, v - \frac{\lambda h \Omega}{2\pi}; x,y) + l(u' - \frac{\lambda h \omega'}{2\pi}, v' - \frac{\lambda h \Omega'}{2\pi}; x+\xi, y+\zeta)] \rangle \\ &\cdot \langle \cos [\omega x + \Omega y + \Psi(\omega, \Omega; u, v; x, y)] \\ &\quad \cdot \cos [\omega'(x+\xi) + \Omega'(y+\zeta) + \Psi(\omega', \Omega'; u', v'; x+\xi, y+\zeta)] \rangle . \quad (12) \end{aligned}$$

It is shown in Appendix B that the last factor in the typical term of the above series expansion reduces to:

$$\begin{aligned} &\delta_{\omega_0} \delta_{\Omega_0} \delta_{\omega'_0} \delta_{\Omega'_0} + \frac{1}{2} \operatorname{Re} \left[\exp i(\omega\xi + \Omega\zeta) \cdot \langle \exp i\Delta\rho^a(x,y;\xi,\zeta) \rangle \right. \\ &\cdot \left. \left[\delta_{u,u'} \delta_{v,v'} \delta_{\omega,\omega'} \delta_{\Omega,\Omega'} + \delta_{u',u - \frac{\lambda h \omega}{2\pi}} \delta_{v',v - \frac{\lambda h \Omega}{2\pi}} \delta_{\omega,-\omega'} \delta_{\Omega,-\Omega'} \right] \right], \quad (13a) \end{aligned}$$

where

$$\begin{aligned} \Delta \rho^a(x, y; \xi, \zeta) &= -\rho^a(u, v; x, y) + \rho^a\left(u - \frac{\lambda h \omega}{2\pi}, v - \frac{\lambda h \Omega}{2\pi}; x, y\right) \\ &+ \rho^a(u, v; x + \xi, y + \zeta) - \rho^a\left(u - \frac{\lambda h \omega}{2\pi}, v - \frac{\lambda h \Omega}{2\pi}; x + \xi, y + \zeta\right) \end{aligned} \quad (13b)$$

is a phase angle which depends upon the differences in the atmospheric phase perturbations at pairs of points.

The first term in Eq. (13a) picks out the "d-c" part (at zero spatial frequency, $\omega = \Omega = \omega' = \Omega' = 0$) of Eq. (12). Upon comparison with Eq. (6) and the change of variables, Eq. (11), this d-c part is seen to be equal to the autocorrelation of $\bar{H}(x, y)$, i. e.:

$$\begin{aligned} \langle \bar{H}(x, y) \bar{H}(x + \xi, y + \zeta) \rangle &= \frac{\tau^2}{4\pi^2 h^4} \sum_{u, v} \Delta u \Delta v P(u, v) \\ &\cdot \sum_{u', v'} \Delta u' \Delta v' P(u', v') \langle \exp [2\ell(u, v; x, y) + 2\ell(u', v'; x + \xi, y + \zeta)] \rangle \\ \xrightarrow[\Delta v \rightarrow 0]{\Delta u \rightarrow 0} \frac{\tau^2}{4\pi^2 h^4} &\left\langle \left[\int_{-\infty}^{\infty} du \int_{-\infty}^{\infty} dv P(u, v) \exp [2\ell(u, v; x, y)] \right] \right. \\ &\cdot \left. \left[\int_{-\infty}^{\infty} du \int_{-\infty}^{\infty} dv P(u, v) \exp [2\ell(u, v; x + \xi, y + \zeta)] \right] \right\rangle \end{aligned} \quad \dots(14)$$

The remainder of Eq. (13) consists of two terms which yield equal contributions¹³ when the summations over u', v', ω' , and Ω' are performed in Eq. (12). Together, these contributions represent the autocorrelation function of $\tilde{H}(x, y)$, i. e.:

$$\begin{aligned} &\langle \tilde{H}(x, y) \tilde{H}(x + \xi, y + \zeta) \rangle \\ &= \langle H(x, y) H(x + \xi, y + \zeta) \rangle - \langle \bar{H}(x, y) \bar{H}(x + \xi, y + \zeta) \rangle \end{aligned}$$

$$\begin{aligned}
 &= \frac{\tau^2 \lambda^2}{16\pi^4 h^2} \operatorname{Re} \int_{-\infty}^{\infty} du \int_{-\infty}^{\infty} dv \int_{-\infty}^{\infty} d\omega \int_{-\infty}^{\infty} d\Omega \exp i(\omega\xi + \Omega\zeta) \\
 &\quad \cdot \langle \exp i\Delta\phi^a(x, y; \xi, \zeta) \rangle P(u, v) P\left(u - \frac{\lambda h \omega}{2\pi}, v - \frac{\lambda h \Omega}{2\pi}\right) \\
 &\quad \cdot \langle \exp \left[\ell(u, v; x, y) + \ell\left(u - \frac{\lambda h \omega}{2\pi}, v - \frac{\lambda h \Omega}{2\pi}; x+\xi, y+\zeta\right) \right. \\
 &\quad \quad \left. + \ell(u, v; x+\xi, y+\zeta) + \ell\left(u - \frac{\lambda h \omega}{2\pi}, v - \frac{\lambda h \Omega}{2\pi}; x+\xi, y+\zeta\right) \right] \rangle .
 \end{aligned}$$

...(15)

(The first equality in Eq. (15) follows from the result,

$$\langle \bar{H}(x, y) \tilde{H}(x+\xi, y+\zeta) \rangle = \langle \tilde{H}(x, y) \bar{H}(x+\xi, y+\zeta) \rangle = 0,$$

which one can show readily.)

In the absence of turbulence ($\ell \rightarrow 0$, $\Delta\phi^a \rightarrow 0$), Eq. (15) expresses the well-known results that the variance of the irradiance is equal to the square of the mean irradiance,^{1,3} $\langle \bar{H}(x, y) \rangle^2 = \bar{H}_0^2$, as required by the negative-exponential irradiance statistics,² and furthermore, that the covariance function of the irradiance distribution is proportional to the two-dimensional Fourier transform of the target autocorrelation function,²⁻⁴ i. e., the far-field diffraction pattern corresponding to the object illumination function.³

When turbulence is present, we consider first the important special case that the entire target lies within a single isoplanatic region.¹⁴ Then we may assume that for any point \vec{p} on the receiver aperture, the complex phase perturbation, $\psi(\vec{p}, \vec{p}') = \ell(\vec{p}, \vec{p}') + i \phi^a(\vec{p}, \vec{p}')$ is the same for all points \vec{p}' on the target. Hence, we may take $\Delta\phi^a(x, y; \xi, \zeta) = 0$ in Eqs. (13)

and (15). Furthermore, although $\ell(u, v; x, y)$ may indeed depend upon the (x, y) coordinates of the receiver aperture, we may take $\ell(u, v; x, y) = \ell(u - \frac{\lambda h \omega}{2\pi}, v - \frac{\lambda h \Omega}{2\pi}; x, y)$, etc., in Eqs. (13), (14) and (15), outside the integrals. Thus, the autocorrelation function of the "noncoherent irradiance", $\bar{H}(x, y)$, reduces to:

$$\begin{aligned} & \langle \bar{H}(x, y) \bar{H}(x+\xi, y+\zeta) \rangle \\ &= \langle \exp [2\ell(\bar{u}, \bar{v}; x, y) + 2\ell(\bar{u}, \bar{v}; x+\xi, y+\zeta)] \rangle \bar{H}_0^2, \end{aligned} \quad (16)$$

where (\bar{u}, \bar{v}) are the coordinates of a typical point on the target, and \bar{H}_0 , the mean irradiance in the absence of turbulence, is given by Eq. (9). Similarly, the spatial autocorrelation function of $\tilde{H}(x, y) = H(x, y) - \bar{H}(x, y)$ becomes:

$$\begin{aligned} & \langle \tilde{H}(x, y) \tilde{H}(x+\xi, y+\zeta) \rangle \\ &= \langle \exp [2\ell(\bar{u}, \bar{v}; x, y) + 2\ell(\bar{u}, \bar{v}; x+\xi, y+\zeta)] \rangle C_H^S(x, y; x+\xi, y+\zeta), \end{aligned} \quad \dots(17)$$

where $C_H^S(x, y; x+\xi, y+\zeta) = \langle \tilde{H}(x, y) \tilde{H}(x+\xi, y+\zeta) \rangle_{\text{non-turbulent}}$

$$\begin{aligned} &= \frac{\pi^2 \lambda^2}{16\pi^4 h^2} \operatorname{Re} \int_{-\infty}^{\infty} d\omega \int_{-\infty}^{\infty} d\Omega \exp i(\omega\xi + \Omega\zeta) \\ & \quad \cdot \int_{-\infty}^{\infty} du \int_{-\infty}^{\infty} dv P(u, v) P(u - \frac{\lambda h \omega}{2\pi}, v - \frac{\lambda h \Omega}{2\pi}) \end{aligned}$$

is the spatial autocovariance of the irradiance fluctuations in the absence of turbulence.^{3, 13}

The common multiplicative factor in Eqs. (16) and (17) arises from the random apodization of the irradiance by the atmospheric turbulence, the same phenomenon which produces scintillation.¹⁰ A similar scintillation-related random apodization (and similar independence of atmospheric phase perturbations)

has been noted in the analysis of Fourier-transform holography in the presence of a random medium.¹⁴⁻¹⁶ The degree of random apodization to be expected in typical situations in the visible and infrared regions will be estimated in the next section.

Finally, if the entire target does not lie within a single isoplanatic region, the ensemble averages in Eqs. (14) and (15) must be evaluated before the integration is performed. Similar ensemble averages arise in estimating the atmospheric modulation noise in an optical heterodyne receiver¹⁷ and in estimating the size of the isoplanatic region in Fourier-transform holography.¹⁵ Although we omit the details here, it is clear that when the target extends beyond a single isoplanatic region, one does not expect to obtain the neat factoring into the product of a target-related part and a turbulence-related part which one finds in Eqs. (16) and (17) for the autocorrelation functions.

Returning to the isoplanatic situation for which Eqs. (16) and (17) apply, let us evaluate the common factor,

$$\begin{aligned}
 F_a &\equiv \langle \exp [2\ell(\bar{u}, \bar{v}; x, y) + 2\ell(\bar{u}, \bar{v}; x+\xi, y+\zeta)] \rangle \\
 &= \langle \exp 2\ell(\bar{u}, \bar{v}; x, y) \rangle \cdot \langle \exp 2\ell(\bar{u}, \bar{v}; x+\xi, y+\zeta) \rangle \\
 &\quad \cdot \exp 4C_\ell(\bar{u}, \bar{v}; x, y; x+\xi, y+\zeta), \\
 &= \exp 4C_\ell(\bar{u}, \bar{v}; x, y; x+\xi, y+\zeta), \tag{18}
 \end{aligned}$$

where the spatial autocovariance of the random function $f(x, y)$

$$\begin{aligned}
 \text{is given by } C_f(x, y; x+\xi, y+\zeta) &= \langle [f(x, y) - \langle f(x, y) \rangle] \\
 &\quad \cdot [f(x+\xi, y+\zeta) - \langle f(x+\xi, y+\zeta) \rangle] \rangle.
 \end{aligned}$$

RIVERSIDE RESEARCH INSTITUTE

The second equality in Eq. (18) follows from the assumption that the log-amplitude, $\ell(u,v;x,y)$, is a Gaussian random variable.^{10,12} $C_\ell(\bar{u},\bar{v};x,y;x+\xi,y+\zeta)$ is the log-amplitude covariance function for a point source at (\bar{u},\bar{v}) . The final equality follows from Eq.(10).

Alternatively, F_a may be expressed in terms of the spatial autocovariance function of the irradiance distribution received in the (x,y) plane from the single point source at (\bar{u},\bar{v}) ,

$$\begin{aligned} C_H^a(x,y;x+\xi,y+\zeta) &= \langle H(x,y) H(x+\xi,y+\zeta) \rangle_{\text{point source}} \\ &\quad - \langle H(x,y) \rangle \langle H(x+\xi,y+\zeta) \rangle \\ &= \bar{H}_0^2 \langle \exp 2\ell(x,y) \rangle \langle \exp 2\ell(x+\xi,y+\zeta) \rangle \\ &\quad \cdot \left[\exp 4C_\ell(\bar{u},\bar{v};x,y;x+\xi,y+\zeta) - 1 \right] \\ &= \bar{H}_0^2 (F_a - 1). \end{aligned} \tag{19}$$

Thus, combining Eqs. (16) and (17), $C_H(x,y;x+\xi,y+\zeta)$, the spatial autocovariance function of the speckled irradiance distribution backscattered from a rough, laser-illuminated target observed through the turbulent atmosphere, is given by:

$$\begin{aligned} C_H(x,y;x+\xi,y+\zeta) &= \langle H(x,y) H(x+\xi,y+\zeta) \rangle \\ &\quad - \langle H(x,y) \rangle \langle H(x+\xi,y+\zeta) \rangle \\ &= \langle \bar{H}(x,y) \bar{H}(x+\xi,y+\zeta) \rangle + \langle \tilde{H}(x,y) \tilde{H}(x+\xi,y+\zeta) \rangle - \bar{H}_0^2 \\ &= \left[\bar{H}_0^2 + C_H^s(x,y;x+\xi,y+\zeta) \right] \exp 4C_\ell(\bar{u},\bar{v};x,y;x+\xi,y+\zeta) - \bar{H}_0^2 \\ &= \bar{H}_0^2 \left\{ \left[1 + \frac{C_H^s(x,y;x+\xi,y+\zeta)}{\bar{H}_0^2} \right] \left[1 + \frac{C_H^a(x,y;x+\xi,y+\zeta)}{\bar{H}_0^2} \right] - 1 \right\} \end{aligned}$$

RIVERSIDE RESEARCH INSTITUTE

so long as the entire target lies within a single isoplanatic region. This equation may be simplified if we assume further that spatial stationarity holds for the separate autocovariances, C_H^S and C_H^a (i. e., for the speckled irradiance in the absence of turbulence^{2,3} as well as for the turbulence-induced irradiance fluctuations from a point source^{5,6,10,12}):

$$\frac{C_H(\xi, \zeta)}{\bar{H}_0^2} = \frac{C_H^S(\xi, \zeta)}{\bar{H}_0^2} + \frac{C_H^a(\xi, \zeta)}{\bar{H}_0^2} + \frac{C_H^S(\xi, \zeta) C_H^a(\xi, \zeta)}{\bar{H}_0^4}. \quad (20)$$

The spatial autocovariance of the speckled irradiance distribution is thus the sum of three terms: a target-related laser-speckle term (Eq. (17)), a term arising from the random apodization by the turbulence, and their product. This result is as expected for the correlation function of the product of two independent random intensity modulation effects.¹⁸

Note that Eq. (20) can be solved in principle for the autocovariance of the target-related speckle alone if $C_H^a(\xi, \zeta)/\bar{H}_0^2$ can be determined from independent measurements.

Relative Magnitudes of Target-Related and Turbulence-Related Contributions

The first term in Eq. (20), $C_H^S(\xi, \zeta)/\bar{H}_0^2$, decreases from unity at $\xi = \zeta = 0$ to zero when $(\xi^2 + \zeta^2)^{1/2}$ exceeds a characteristic "speckle size". It is clear from Eq. (17) that this speckle size is inversely proportional to a target-related dimension (e. g., its maximum transverse dimension if the target reflects uniformly and is uniformly illuminated).¹⁻⁴

RIVERSIDE RESEARCH INSTITUTE

The second term in Eq. (20) gives the covariance of the turbulence-induced irradiance fluctuations measured for a point source with a pair of point receivers separated by (ξ, ζ) . When $\xi = \zeta = 0$, $C_H^a(\xi, \zeta) / \bar{H}_0^2$ becomes σ_H^2 / \bar{H}_0^2 , which is more commonly written as σ_I^2 / \bar{I}^2 and called the (normalized) intensity variance.^{10, 12} $C_H^a(\xi, \zeta) / \bar{H}_0^2$ decreases from its maximum value of σ_I^2 / \bar{I}^2 at $\xi = \zeta = 0$ to zero when $(\xi^2 + \zeta^2)^{1/2}$ exceeds a correlation length of the order of $(\lambda L)^{1/2}$, where L is on the order of the path length through uniform turbulence (e. g., horizontal propagation),^{10, 19-21} and on the order of the height to the tropopause for vertical propagation.^{10, 19}

For near-horizontal propagation under "saturation-of-scintillation" conditions,¹⁰

$$\sigma_I^2 / \bar{I}^2 \approx 10. \quad (\text{"Saturation"})$$

Thus, except for large values of (ξ, ζ) and speckle sizes much larger than $(\lambda L)^{1/2}$, the covariance is dominated by the second term in Eq. (20) under these adverse turbulence conditions. The observed irradiance fluctuations are mainly due to the scintillation-related random apodization.

On the other hand, for vertical propagation in the visible, it is known from stellar scintillation data¹⁹ that

$$\sigma_I^2 / \bar{I}^2 \approx 0.2. \quad (\text{Visible astronomy; vertical path})$$

Furthermore, available data at 10.6 μm wavelength²⁰⁻²² are in agreement with scaling the visible scintillation data according

RIVERSIDE RESEARCH INSTITUTE

to $\lambda^{-7/8}$, i. e.,

$$\sigma_I^2 / \bar{I}^2 \approx 0.008. \quad (10.6 \mu\text{m}; \text{vertical path at night}^{23})$$

Consequently, the autocovariance of the irradiance distribution obtained at 10.6 μm from a near-zenith exoatmospheric target will be dominated strongly by the first term in Eq. (20). The observed irradiance fluctuations are mainly target-related laser speckles. The autocorrelation function of the speckle pattern is proportional to the Fourier transform of the target autocorrelation function, with only a weak dependence on the turbulence-induced random apodization.

And for near-zenith targets in the visible region, one's ability to sort out the contributions from each of the three terms in Eq. (20) will depend upon the relative sizes of $(\lambda L)^{1/2}$ and the speckle size, as well as upon the degree of turbulence, slant range, and zenith angle. Based on the measurements of "shadow bands" in stellar astronomy, $(\lambda L)^{1/2}$ can be expected to vary from 3 or 4 to 7 or 8 cm in the visible.¹⁰ For small zenith angles, σ_I^2 / \bar{I}^2 varies as $\sec^p \theta$, where θ is the zenith angle, and p is a number on the order of unity.¹⁹

The size of the isoplanatic region is difficult to estimate, although guesses of $\approx 10^{-4}$ rad for near-zenith exoatmospheric objects are common. (Even crude experimental data are available only for near-horizontal propagation.^{15, 16}) The present theory thus is likely to be appropriate for targets with transverse dimensions of meters at ranges of 10 km or greater.

RIVERSIDE RESEARCH INSTITUTE

Power Spectral Density of the Irradiance Distribution

By the Wiener-Khinchin theorem,²⁴ the power spectral density of the irradiance distribution at the receiver aperture is given by the two-dimensional Fourier transform of the spatial autocorrelation function (assumed to be spatially stationary). Thus, the power spectral density, $S(\omega, \Omega)$, is given by the Fourier transform of $\langle H(x, y) H(x+\xi, y+\zeta) \rangle$. In the absence of turbulence, from Eqs. (16) and (17),

$$S(\omega, \Omega) = S_0(\omega, \Omega) = \bar{H}_0^2 \delta(\omega) \delta(\Omega) + \frac{\tau^2 \lambda^2}{16\pi^4 h^2} \int_{-\infty}^{\infty} du \int_{-\infty}^{\infty} dv P(u, v) P(u - \frac{\lambda h \omega}{2\pi}, v - \frac{\lambda h \Omega}{2\pi}), \dots (21)$$

where $\delta(x)$ is the Dirac delta function, and

\bar{H}_0^2 is the square of the mean irradiance.

(The "lag" variables, ξ and ζ , are assumed to range from $-\infty$ to $+\infty$. This is appropriate when the aperture contains several correlation "widths".) Thus, in the absence of turbulence, the power spectral density of the received irradiance pattern is the sum of a fixed known (delta) function and the target correlogram, i. e., the spatial autocorrelation function of the reflected irradiance distribution at the target.^{2, 3, 13}

In the presence of an intervening turbulent atmosphere, the power spectral density may be calculated straightforwardly, by means of Eqs. (16)-(20), when the entire target is situated in one isoplanatic region. Denoting results in the absence of

RIVERSIDE RESEARCH INSTITUTE

turbulence by zero subscripts, the power spectral density is given by:

$$S(\omega, \Omega) = \mathcal{F} \{ \exp 4C_r(\xi, \zeta) \} * S_0(\omega, \Omega) \quad (22)$$

$$= S_0(\omega, \Omega) + \mathcal{F} \left\{ \frac{C_H^a(\xi, \zeta)}{\bar{H}_0^2} \right\} * S_0(\omega, \Omega), \quad (23)$$

where $S_0(\omega, \Omega)$ is given by Eq. (21),

* denotes the convolution (or Faltung) operation, and \mathcal{F} denotes the two-dimensional Fourier transform.

The convolution operation arises because the Fourier transform of the product of $\exp 4C_r(\xi, \zeta)$ and the correlation function in the non-turbulent case is given by the convolution of their Fourier transforms.

In general, the power spectral density in Eq. (23) is the sum of two terms. The first term is the uncorrupted $S_0(\omega, \Omega)$, which contains all of the "fine structure" which may be present in the target correlogram. The second term is a blurred version of $S_0(\omega, \Omega)$, obtained by convolving it with the spectrum of the turbulence-induced random apodization. The "energy" contained in this second term is $C_H^a(0,0)/\bar{H}_0^2$ (i. e., σ_I^2/\bar{I}^2) times that in the first term.

As noted earlier, for vertical propagation at $10.6 \mu\text{m}$, $\sigma_I^2/\bar{I}^2 \ll 1$, so that the first term in Eq. (23) is dominant, and $S(\omega, \Omega)$ reduces to $S_0(\omega, \Omega)$ to a very good approximation. In other cases, where turbulent effects are significant but can be determined from independent measurements, then the spectrum of

the random apodization is known. Thus, $S_o(\omega, \Omega)$ can still be obtained.

In any event, the second term in Eq. (20) is determined by the relative sizes of the turbulence-related correlation length, $\rho_o = (\lambda L)^{1/2}$, and the characteristic speckle dimensions. If the uniformly reflecting target is of irregular shape, the speckle dimension along any given direction is related to the angular subtense, θ_t , of the target along that direction by $d_s \sim \lambda/\theta_t$, where d_s is the width of the covariance function of the irradiance distribution, $C_H^S(\xi, \zeta)$, Eq. (17). A feature related to θ_t will exist in the target correlogram, and hence in the power spectrum, $S_o(\omega, \Omega)$, Eq. (21), at a distance from (0,0) which is inversely proportional to the speckle size, d_s . Even in the visible region, in the limit that the speckle sizes are much larger than the scintillation-related length, $\rho_o = (\lambda L)^{1/2}$, $S(\omega, \Omega)$ in Eq. (23) reduces to $S_o(\omega, \Omega)$, unchanged. Physically, $S_o(\omega, \Omega)$ emerges in this case because the turbulence-induced irradiance fluctuations are effectively aperture-averaged (i. e., low-pass filtered) to zero within a single speckle cell.^{10, 19} Thus, target information contained in the larger speckle sizes is retained in the power spectral density, uncorrupted by the turbulence.

In the limit that the speckle sizes are much smaller than ρ_o , Eq. (23) becomes:

$$S(\omega, \Omega) \xrightarrow{\sqrt{\lambda L} \gg \lambda/\theta_t} (1 + \sigma_I^2 / \bar{I}^2) S_o(\omega, \Omega). \quad (24)$$

RIVERSIDE RESEARCH INSTITUTE

In this limit, the relatively narrow spectrum of the scintillation imposes a uniform apodization across the speckle power spectrum. The power spectral density becomes dependent upon the variance of the turbulence-induced irradiance fluctuations. This variance itself is subject to a large variance,^{10,19-22} Thus, if the speckle sizes are smaller than $(\lambda L)^{1/2}$, the structure of the power spectral density is unaffected by the turbulence, but its overall strength is subject to strong random fading from look to look in the visible. The random fading is negligible at 10.6 μm for exoatmospheric objects observed near the zenith at night, for the factor multiplying $S_o(\omega, \Omega)$ in Eq. (24) differs from unity by less than 1%.

We conclude that, in favorable cases, so long as the entire target lies within a single isoplanatic region, the power spectral density, properly computed, is equal to the sum of a fixed, known function and the target correlogram, Eq. (21), just as in the absence of turbulence.

RIVERSIDE RESEARCH INSTITUTE

Summary

Through the use of the extended Huygens-Fresnel principle, we have calculated the autocovariance and power spectral density of the irradiance distribution backscattered from a rough, laser-illuminated target observed through the turbulent atmosphere. For the special case where the entire target lies within a single isoplanatic region, and where the correlation length of the surface roughness distribution is not resolved by the receiving aperture, we verified that the autocovariance of the irradiance (normalized to the square of the mean irradiance) becomes the sum of three terms: the normalized covariance in the absence of turbulence (i. e., the Fourier transform of the target correlogram), the normalized covariance of the point-source irradiance arising from the turbulence-induced random apodization, and their product. The power spectral density of the received irradiance is then the sum of the uncorrupted, turbulence-free spectrum (proportional to the target correlogram) and a blurred version of this spectrum, obtained by convolution with the spectrum of the random apodization produced by the turbulence. We noted that, in principle, when the normalized autocovariance function of the random apodization is known, both the target correlogram and its Fourier transform may be determined explicitly from the statistics of the irradiance distribution. Finally, when experimental data on stellar scintillation were combined with known data at $10.6 \mu\text{m}$, we concluded

RIVERSIDE RESEARCH INSTITUTE

that the effect of the random apodization will be negligibly small for a ground-based receiver observing a suitable near-zenith exoatmospheric target illuminated at $10.6 \mu\text{m}$.

Acknowledgments

The authors wish to thank Marek Elbaum for his helpful suggestions and criticisms. The research reported here was sponsored by the Defense Advanced Research Projects Agency and was administered by the Air Force Electronics Systems Division under Contract No. F19628-71-C-0162.

RIVERSIDE RESEARCH INSTITUTE

Appendix A

In this Appendix, we calculate the ensemble mean, $\langle \tilde{H}(x,y) \rangle$, i. e., the average of $\tilde{H}(x,y)$ over all possible realizations of the random variables, ℓ , ϕ^a , and ϕ^s . The ensemble mean of a typical term in Eq. (7) contains a factor of the form

$$\begin{aligned} Q(u,v;u',v';x,y) &= Q(\vec{p}_1; \vec{p}_2; \vec{p}) \\ &= \langle \exp [\ell(\vec{p}_1; \vec{p}) + \ell(\vec{p}_2; \vec{p})] \cos \left[\frac{k}{h}(\vec{p}_1 - \vec{p}_2) \cdot \vec{p} \right. \\ &\quad \left. + \phi^s(\vec{p}_1) - \phi^s(\vec{p}_2) + \phi^a(\vec{p}_1; \vec{p}) - \phi^a(\vec{p}_2; \vec{p}) \right] \rangle \end{aligned}$$

where $\vec{p}_1 = (u, v, 0)$, $\vec{p}_2 = (u', v', 0) = (u - \frac{\lambda h \omega}{2\pi}, v - \frac{\lambda h \Omega}{2\pi}, 0)$, and

$$\vec{p} = (x, y, h), \text{ so that, e. g., } \frac{k}{h}(\vec{p}_1 - \vec{p}_2) \cdot \vec{p} = \omega x + \Omega y.$$

If we assume that ℓ , ϕ^a , and ϕ^s are effectively uncorrelated, i. e., that $\ell(\vec{p}_1; \vec{p}) + \ell(\vec{p}_2; \vec{p})$ is independent of $\phi^s(\vec{p}_1) - \phi^s(\vec{p}_2)$ as well as of $\phi^a(\vec{p}_1; \vec{p}) - \phi^a(\vec{p}_2; \vec{p})$, then

$$\begin{aligned} Q(\vec{p}_1; \vec{p}_2; \vec{p}) &= \langle \exp [\ell(\vec{p}_1; \vec{p}) + \ell(\vec{p}_2; \vec{p})] \rangle \text{Re} \left[\exp \frac{ik}{h}(\vec{p}_1 - \vec{p}_2) \cdot \vec{p} \right. \\ &\quad \left. \cdot \langle \exp i [\phi^s(\vec{p}_1) - \phi^s(\vec{p}_2)] \rangle \cdot \langle \exp i [\phi^a(\vec{p}_1; \vec{p}) - \phi^a(\vec{p}_2; \vec{p})] \rangle \right] \\ &\dots(A.1) \end{aligned}$$

We shall show that, according to our target model,

$$\langle \exp i [\phi^s(\vec{p}_1) - \phi^s(\vec{p}_2)] \rangle = \delta_{\vec{p}_1, \vec{p}_2} = \delta_{\omega_0} \delta_{\Omega_0} \dots(A.2)$$

Then (A.1) becomes

$$Q(\vec{p}_1; \vec{p}_2; \vec{p}) = Q(\vec{p}_1; \vec{p}_1; \vec{p}) \delta_{\vec{p}_1, \vec{p}_2} = \langle \exp [2\ell(\vec{p}_1; \vec{p})] \rangle \delta_{\omega_0} \delta_{\Omega_0}$$

RIVERSIDE RESEARCH INSTITUTE

or:

$$\Omega(\vec{p}_1; \vec{p}_2; \vec{p}) = \langle \exp [2\mathcal{L}(u, v; x, y)] \rangle \delta_{\omega_0} \delta_{\Omega_0} \quad \dots (A.3)$$

Thus, summing over (ω, Ω) in the ensemble average of Eq. (7), we obtain $\langle \tilde{H}(x, y) \rangle = 0$, i. e., Eq. (8). It remains for us to show that (A.2) holds.

For $f_1 = \phi^S(\vec{p}_1)$ and $f_2 = \phi^S(\vec{p}_2)$ real, jointly Gaussian random variables, it follows that

$$\begin{aligned} \langle \exp i(f_1 \pm f_2) \rangle &= \exp i\langle f_1 \rangle \exp i\langle \pm f_2 \rangle \\ &\cdot \exp \left[-\frac{1}{2} [\text{Var}(f_1) + \text{Var}(f_2) \pm 2 \text{Cov}(f_1, f_2)] \right], \end{aligned} \quad \dots (A.4)$$

where $\text{Var}(f_j) = \langle (f_j - \langle f_j \rangle)^2 \rangle = \langle f_j^2 \rangle - \langle f_j \rangle^2$, $j = 1, 2$,

$$\text{Cov}(f_1, f_2) = \text{Cov}(f_2, f_1) = \langle (f_1 - \langle f_1 \rangle)(f_2 - \langle f_2 \rangle) \rangle.$$

By our assumption⁷ that the correlation length between individual scatterers is smaller than the resolution limit of the receiver aperture, we may take $\text{Cov}(f_1, f_2) = \text{Var}(f_1) \delta_{\vec{p}_1, \vec{p}_2}$ with negligible error. Thus, for $\vec{p}_1 \neq \vec{p}_2$,

$$\begin{aligned} \langle \exp i [\phi^S(\vec{p}_1) - \phi^S(\vec{p}_2)] \rangle &= \exp i\langle \phi^S(\vec{p}_1) \rangle \\ &\cdot \exp -i\langle \phi^S(\vec{p}_2) \rangle \exp \left[-\frac{1}{2} [\text{Var}(f_1) + \text{Var}(f_2)] \right]. \end{aligned}$$

Finally, we have assumed that the standard deviation of ϕ^S is at least equal to π ,⁸ so that the above expression is bounded by $e^{-\pi^2} = 5.17 \cdot 10^{-5}$, effectively zero. (A.2) follows.

RIVERSIDE RESEARCH INSTITUTE

In the more general case that p_s , the correlation length between the individual scatterers, is resolved, both the back-scattered irradiance and its covariance will depend upon $\text{Cov}(f_1, f_2)$.^{2, 25-28} Formally, if we assume a Gaussian phase distribution, so that Eq. (A-4) applies, and we suppose that $\langle f_1 \rangle = \langle f_2 \rangle$, $\text{Var}(f_1) = \text{Var}(f_2) = \sigma^2$, and $\text{Cov}(f_1, f_2) = \sigma^2 C_s(\Delta p')$, where $\Delta p' = |\vec{p}_1 - \vec{p}_2|$ and $C_s(\Delta p')$ is the normalized autocovariance function of the surface roughness distribution,²⁸ we obtain in place of Eq. (A.2):

$$\begin{aligned} \langle \exp i [\phi^s(\vec{p}_1) - \phi^s(\vec{p}_2)] \rangle &= \exp - \left[\sigma^2 [1 - C_s(\Delta p')] \right] \\ &= \exp - \left[\sigma^2 \left[1 - C_s\left(\frac{\lambda h \omega}{2\pi}, \frac{\lambda h \Omega}{2\pi}\right) \right] \right], \end{aligned} \quad \dots(A.5)$$

where $C_s(\Delta p')$ is nearly unity for $\Delta p' \ll p_s$, and nearly zero for $\Delta p' \gg p_s$. The additional complexity introduced by Eq. (A.5) is unwarranted in the many practical cases in which p_s is unresolved.²

However, it should be pointed out that $\text{Var}(f_1)$ may be less than π if the target is only slightly rough (i. e., imperfectly specular). Then the ensemble mean, $\langle \tilde{H}(x, y) \rangle$, may very well not be zero, and the usual assumption of spatial stationarity^{2, 25-27} may break down.²⁸

RIVERSIDE RESEARCH INSTITUTE

Appendix B

The typical term in Eq. (12) contains as a factor the ensemble mean,

$$\langle \cos [\omega x + \Omega y + \Psi(\omega, \Omega; u, v; x, y)] \cdot \cos [\omega'(x+\xi) + \Omega'(y+\zeta) + \Psi(\omega', \Omega'; u', v'; x+\xi, y+\zeta)] \rangle, \quad (\text{B.1})$$

which we wish to evaluate. If we apply the trigonometric identity, $\cos a \cos b = \frac{1}{2} \text{Re} [\exp i(a - b) + \exp i(a + b)]$, the factor (B.1) becomes:

$$\begin{aligned} & \frac{1}{2} \text{Re} \left[\exp i [(\omega - \omega')x + (\Omega - \Omega')y - \omega'\xi - \Omega'\zeta] \right. \\ & \quad \cdot \langle \exp i [\Psi(\omega, \Omega; u, v; x, y) - \Psi(\omega', \Omega'; u', v'; x+\xi, y+\zeta)] \rangle \\ & \quad + \exp i [(\omega + \omega')x + (\Omega + \Omega')y + \omega'\xi + \Omega'\zeta] \\ & \quad \left. \cdot \langle \exp i [\Psi(\omega, \Omega; u, v; x, y) + \Psi(\omega', \Omega'; u', v'; x+\xi, y+\zeta)] \rangle \right] \\ & \hspace{15em} \dots(\text{B.2}) \end{aligned}$$

However, since ϕ^a and ϕ^s are obviously independent real random variables, the averages in (B.2) become:

$$\begin{aligned} & \langle \exp i [\Psi(\omega, \Omega; u, v; x, y) \mp \Psi(\omega', \Omega'; u', v'; x+\xi, y+\zeta)] \rangle \\ & = \langle \exp i \left[\phi'^s(u, v) \mp \phi'^s(u', v') - \phi'^s\left(u - \frac{\lambda h \omega}{2\pi}, v - \frac{\lambda h \Omega}{2\pi}\right) \right. \\ & \quad \left. \pm \phi'^s\left(u' - \frac{\lambda h \omega'}{2\pi}, v' - \frac{\lambda h \Omega'}{2\pi}\right) \right] \rangle \\ & \cdot \langle \exp i \left[\phi^a(u, v; x, y) \mp \phi^a(u', v'; x+\xi, y+\zeta) \right. \\ & \quad \left. - \phi^a\left(u - \frac{\lambda h \omega}{2\pi}, v - \frac{\lambda h \Omega}{2\pi}; x, y\right) \pm \phi^a\left(u' - \frac{\lambda h \omega'}{2\pi}, v' - \frac{\lambda h \Omega'}{2\pi}; x+\xi, y+\zeta\right) \right] \rangle. \\ & \hspace{15em} \dots(\text{B.3}) \end{aligned}$$

RIVERSIDE RESEARCH INSTITUTE

By a "stationary-phase" argument, similar to that used to obtain Eq. (A.2) in Appendix A, we are led to the assertion that, according to our target model,⁷

$$\langle \exp i [\phi'^S(\vec{p}_1) - \phi'^S(\vec{p}_2) + \phi'^S(\vec{p}_3) - \phi'^S(\vec{p}_4)] \rangle = 0,$$

unless the phases in square brackets cancel to zero. This cancellation occurs either when

$$\vec{p}_1 = \vec{p}_2 \quad \text{and} \quad \vec{p}_3 = \vec{p}_4 \quad (\text{condition } \underline{a})$$

or when

$$\vec{p}_1 = \vec{p}_4 \quad \text{and} \quad \vec{p}_2 = \vec{p}_3 \quad (\text{condition } \underline{b}).$$

For the upper sign in (B.3), we identify $\vec{p}_1 = (u, v)$, $\vec{p}_2 = (u - \frac{\lambda h \omega}{2\pi}, v - \frac{\lambda h \Omega}{2\pi})$, $\vec{p}_3 = (u' - \frac{\lambda h \omega'}{2\pi}, v' - \frac{\lambda h \Omega'}{2\pi})$, $\vec{p}_4 = (u', v')$.

Then condition a corresponds to $\omega = \Omega = \omega' = \Omega' = 0$, and condition b corresponds to $u = u'$, $v = v'$, $\omega = \omega'$, $\Omega = \Omega'$. For the lower sign in (B.3), interchange the correspondences of \vec{p}_3 and \vec{p}_4 , i. e., $\vec{p}_3 = (u', v')$, $\vec{p}_4 = (u' - \frac{\lambda h \omega'}{2\pi}, v' - \frac{\lambda h \Omega'}{2\pi})$. Then the condition a again corresponds to $\omega = \Omega = \omega' = \Omega' = 0$, and condition b corresponds to $u' = u - \frac{\lambda h \omega}{2\pi}$, $v' = v - \frac{\lambda h \Omega}{2\pi}$, $\omega = -\omega'$, $\Omega = -\Omega'$. (These negative-frequency possibilities were overlooked in Ref. 3, making Eq. (17) of that paper too small by a factor of 2.)

Substituting the non-zero values of Eq. (B.3) into (B.2), and noting that $\text{Re exp}(ia) = \text{Re exp}(-ia)$, we are led immediately to Eq. (13).

RIVERSIDE RESEARCH INSTITUTE

As discussed in Appendix A, the additional complexity introduced when the correlation function of the surface roughness distribution is taken into account explicitly^{2,2 -2} is not warranted when the correlation length, p_s , is not resolved by the aperture.⁷ However, the calculation is straightforward if $\phi^S(\vec{p}')$ is Gaussian-distributed and the entire target lies in a single isoplanatic region.

RIVERSIDE RESEARCH INSTITUTE

REFERENCES

1. J. D. Rigden and E. I. Gordon, Proc. I. R. E. 50, 2367 (1962).
2. J. W. Goodman, "Statistical Properties of Laser Sparkle Patterns," Tech. Rept. SEL-63-140 (TR 2303-1), Stanford Univ. Electronics Lab, Stanford, Cal., Dec. 1963; Proc. I. E. E. E. 53, 1688 (1965).
3. L. I. Goldfischer, J. Opt. Soc. Amer., 55, 247 (1965).
4. P. Hariharan, Optica Acta 19, 791 (1972).
5. R. F. Lutomirski and H. T. Yura, Appl. Optics 10, 1652 (1971).
6. H. T. Yura, Appl. Optics 11, 1399 (1972).
7. In this paper, we restrict our attention to the situation in which the correlation length between individual scatterers is much less than the smallest separation which a telescope with the given aperture can resolve: $\approx \lambda h/D_{\text{tel}}$. The observation point may be in the near field of the target as a whole, but it must be in the far field of this correlation length.
8. This assumption is essentially equivalent to that of Ref. 3 in which $\phi^S(u, v)$ is taken to be uniformly distributed in the interval $(0, 2\pi)$, as discussed, e. g., in Ref. 9. The Gaussian assumption permits the generalizations discussed in the Appendices.

RIVERSIDE RESEARCH INSTITUTE

9. B. L. McGlamery, "Image Restoration Techniques Applied to Astronomical Photography," in Astronomical Use of TV-Type Image Sensors, NASA SP-256, V. R. Boscarino, Ed., Washington, D. C., 1971, especially pp. 175-179.
10. R. S. Lawrence and J. W. Strohbehn, Proc. IEEE 58, 1523 (1970).
11. Cf. W. Martienssen and E. Spiller, Amer. J. Phys. 32, 919 (1964).
12. D. L. Fried, J. Opt. Soc. Amer. 57, 169 (1967).
13. Eq. (17) of Ref. 3 is in error by a factor of two. The error arises from the omission of the negative-frequency contributions which give rise to the second string of Kronecker deltas in our Eq. (13). See Appendix B.
14. J. W. Goodman, "Analysis of Wavefront-Reconstruction Imaging through Random Media," in Restoration of Atmospherically Degraded Images, Vol. 2, Woods Hole Summer Study, National Academy of Sciences, National Research Council, Washington, D. C., July 1966. See also J. Opt. Soc. Amer. 60, 506 (1970).
15. J. D. Gaskill, J. Opt. Soc. Amer. 58, 600 (1968); 59, 308 (1969).
16. H. T. Yura, Appl. Optics 12, 1188 (1973).
17. D. L. Fried, IEEE J. Quantum Electron. QE-3, 213 (1967).
18. We thank an anonymous reviewer for suggesting this observation.
19. V. I. Tatarskii, The Effects of the Turbulent Atmosphere

RIVERSIDE RESEARCH INSTITUTE

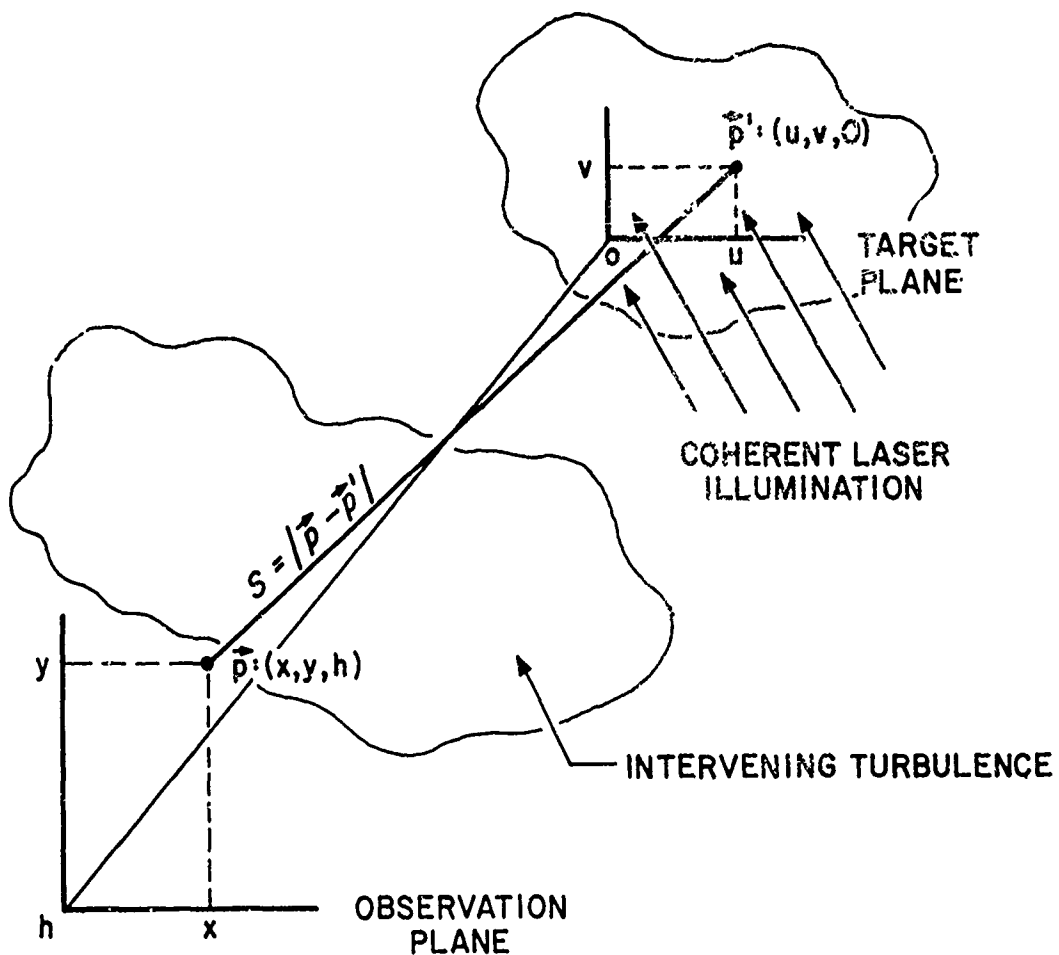
- on Wave Propagation, Israel Program for Scientific Translations, Jerusalem, 1971. (Available from National Technical Information Service, Springfield, Va. 22151.)
20. M. W. Fitzmaurice, J. L. Bufton, and P. O. Minott, J. Opt. Soc. Amer. 59, 7 (1969).
 21. J. R. Kerr, J. Opt. Soc. Amer. 62, 1040 (1972).
 22. D. P. Woodman, M. Boehme, C. Brown, A. Kraemer, P. Titterton, P. Minott, M. Fitzmaurice, and J. Bufton, IEEE J. Quantum Electron. QE-7, 273 (1971).
 23. Daytime variances can be expected to be an order of magnitude higher, according to calculations by R. F. Lutomirski (private communication).
 24. A. M. Yaglom, An Introduction to the Theory of Stationary Random Functions, translated by R. A. Silverman, Prentice-Hall, 1962.
 25. R. B. Crane, J. Opt. Soc. Amer. 60, 1658 (1970).
 26. D. P. Greenwood and E. J. Powers, Jr., IEEE Trans. AP-20, 19 (1972).
 27. P. H. Deitz and F. Paul Carlson, J. Opt. Soc. Amer. 63, 274 (1973).
 28. M. Elbaum, M. Greenebaum, and M. King (in preparation).

RIVERSIDE RESEARCH INSTITUTE

FIGURE CAPTION

Fig. 1: An exoatmospheric target is illuminated with coherent laser light. The scattered light passes through the turbulent atmosphere to the ground-based receiver telescope. The irradiance in the aperture is recorded at each point (x,y) .

RIVERSIDE RESEARCH INSTITUTE



RIVERSIDE RESEARCH INSTITUTE

Paper No. 4

THE RESIDUAL EFFECTS OF ATMOSPHERIC TURBULENCE
ON A CLASS OF HOLOGRAPHIC IMAGING AND CORRELOGRAPHY SYSTEMS

(This paper was presented at the Topical Meeting on Optical Propagation Through Turbulence. The abstract on the first four pages appears in the Digest of Technical Papers given at the meeting.⁷ The Vu-Graphs used are reproduced here following the abstract. Research Note N-6/174-3-33 contained an earlier version of some of this material.³)

Both laser correlography and on-axis lensless Fourier-transform holography are treated in this paper. The effects of using a ground-based laser illuminator are taken into consideration. CO₂ laser correlography systems are shown to be particularly insensitive to turbulence-caused degradation of performance against space objects, although a valid verification experiment cannot be performed over ground-level horizontal propagation paths.

Paper Th A6 of the Topical Meeting on Optical Propagation Through Turbulence, July 9-11, 1974, Boulder, Colorado.

THE RESIDUAL EFFECTS OF ATMOSPHERIC TURBULENCE
ON A CLASS OF HOLOGRAPHIC IMAGING AND CORRELOGRAPHY SYSTEMS⁺

Michael Greenebaum

Riverside Research Institute
New York, N. Y. 10023

Recent results concerning the spatial covariance of scintillations are used to estimate the effects of turbulence on holographic imaging and laser correlography systems.

In this paper, we use recent experimental and theoretical results on the spatial covariance of turbulence-induced scintillations to estimate the residual effects of turbulence on Fourier-transform holographic imaging and on laser correlography systems. In marked contrast to ordinary imaging, both lensless Fourier-transform holography^{1,2} and laser correlography^{3,4} are immune to the phase perturbations introduced by turbulence. This is true as long as the entire object lies well within a single isoplanatic region.^{1,4} In particular, it is well known³ that the two-dimensional Wiener spectrum of the speckled irradiance distribution scattered from a coherently illuminated object

⁺ Research sponsored by the Defense Advanced Research Projects Agency under Contract No. F19628-71-C-0162.

RIVERSIDE RESEARCH INSTITUTE

is proportional to the "correlogram" of the object illumination function. We have shown previously⁴ that, for a ground-based receiver observing an exoatmospheric object smaller than the isoplanatic patch, the phase perturbations produced by the turbulence do not affect this result. (The relevant isoplanatic patch size is estimated to be about 10 μ rad in angular extent.) The only residual effect of the turbulence is a random apodization of the irradiance.⁴ Goodman¹ has shown that, under similar isoplanatic patch conditions, a similar result holds for lensless Fourier-transform holographic imaging. Thus, in each of these "phase-insensitive" systems, estimates of the random apodization are of paramount importance.

Because of past difficulties in understanding the behavior of the covariance of scintillations in the region of strong turbulence,⁵⁻⁸ it has been necessary in earlier treatments to restrict the system calculation, at least implicitly, to cases where $\sigma_x^2 \lesssim 0.3$.^{4,9} It has been shown quite recently¹⁰ that it is possible to explain the experimental results in the saturation region, $\sigma_x^2 > 0.3$, in a quantitative manner by means of approximate calculations based on coherence-degradation arguments. In the present paper, we use similar arguments to predict, at least semi-quantitatively, the behavior of holographic imaging and laser correlography in the region of strong turbulence. (At large angles from the zenith direction, strong turbulence will be encountered even in the infrared.)

RIVERSIDE RESEARCH INSTITUTE

Secondly, earlier analyses^{1, 2, 4, 9} have considered explicitly the turbulence effects in the "down-link" only, i. e., from the uniformly illuminated exoatmospheric object to the ground. Here, we also consider the complications introduced when a ground-based laser illuminator must be used; i. e., "up-link" turbulence effects are included.

In particular, we can express the results of our analysis of laser correlography in terms of $C_{\text{usd}}(\vec{\rho})$, the normalized spatial covariance of the irradiances measured at two points separated by distance $\vec{\rho}$ in the entrance pupil of the receiver. (The approximation of spatial stationarity is made.) The measured irradiance, a stochastic quantity, is related to the transmitted laser power by three random, independent amplitude-modulation processes, so that:

$$C_{\text{usd}}(\vec{\rho}) = C_{\text{u}}(\vec{\rho}) + C_{\text{s}}(\vec{\rho}) + C_{\text{d}}(\vec{\rho}) + C_{\text{u}}(\vec{\rho}) C_{\text{s}}(\vec{\rho}) + C_{\text{s}}(\vec{\rho}) C_{\text{d}}(\vec{\rho}) \\ + C_{\text{d}}(\vec{\rho}) C_{\text{u}}(\vec{\rho}) + C_{\text{u}}(\vec{\rho}) C_{\text{s}}(\vec{\rho}) C_{\text{d}}(\vec{\rho}), \quad \dots(1)$$

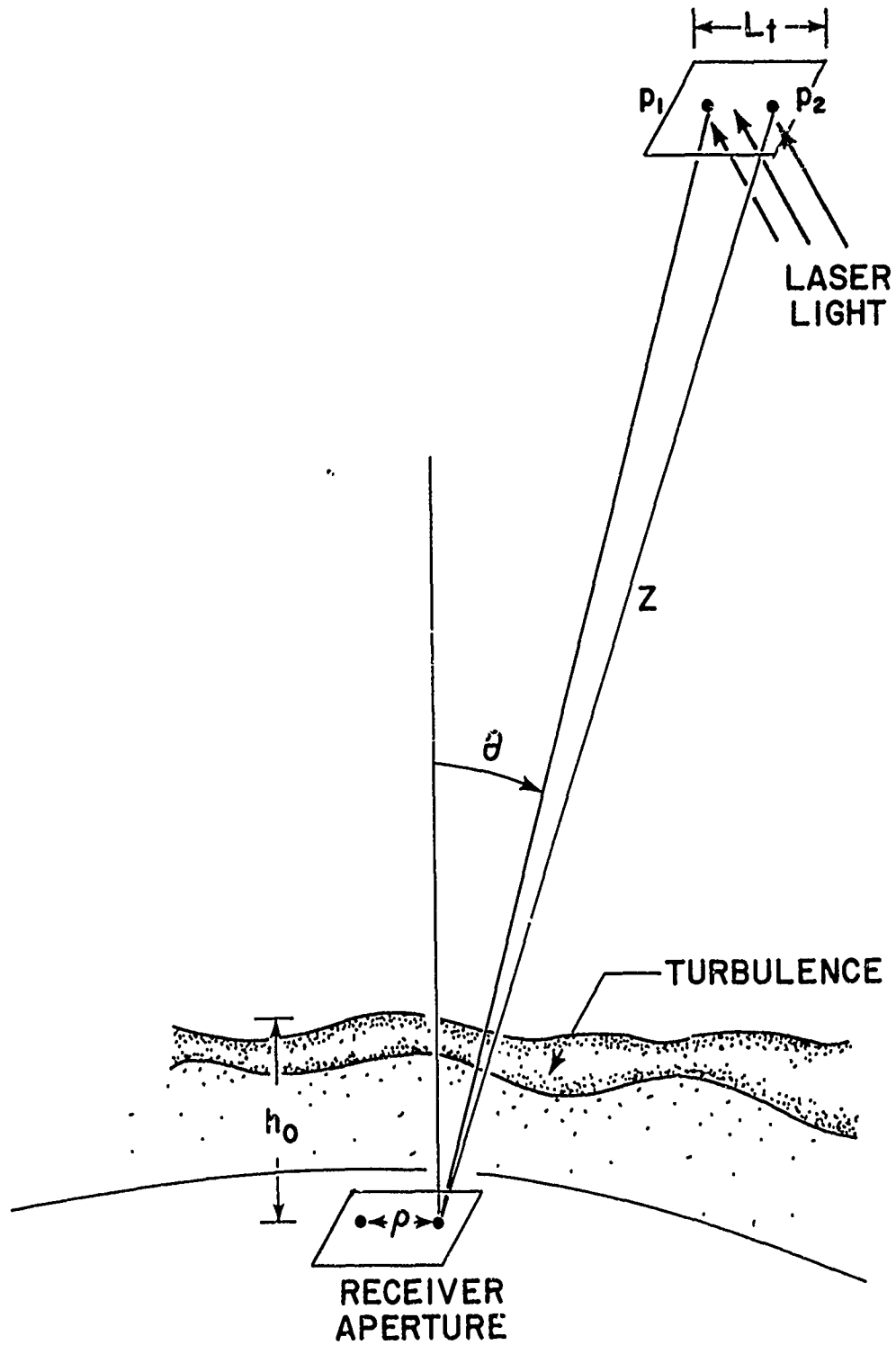
where $C_{\text{u}}(\vec{\rho})$, $C_{\text{s}}(\vec{\rho})$, and $C_{\text{d}}(\vec{\rho})$ are the normalized covariances of the received irradiance which would be obtained if only one of these three processes were present separately. (The u, s, and d subscripts relate to "up-link" turbulence, laser "speckles", and "down-link" turbulence, respectively.) In particular, the term of direct interest in correlography is $C_{\text{s}}(\vec{\rho})$, the autocovariance of the "speckles" which would be observed in the absence of turbulence. If the scattering object is a uniformly reflecting

RIVERSIDE RESEARCH INSTITUTE

rectangle of width L_t , for example, the characteristic width of C_s will be $\lambda z/L_t$ (a relationship similar to the van Cittert-Zernike theorem).^{3,4} (The Fourier transform of C_s is the correlogram of the object.) $C_u(\vec{\rho}) \approx C_u(0)$ is the autocovariance of those irradiance fluctuations at the receiver which arise from fluctuations in the object illumination caused by scintillation and beam wander.^{6,11} $C_d(\vec{\rho})$ is the normalized autocovariance of turbulence-induced scintillations for a monochromatic point source at the location of the object.^{4,5,8,10} The behavior and influence of C_u and C_d upon one's ability to retrieve the object-related information contained in C_s are discussed both in the weak- and strong-turbulence regimes, using techniques similar to Ref. 10. It is shown that a large receiver aperture operating with 10- μ m laser illumination can obtain relatively "clean" correlograms of near-zenith exoatmospheric objects, and that lensless Fourier-transform holography is also feasible.

References

1. J. W. Goodman, "Analysis of Wavefront-Reconstruction Imaging through Random Media," in Restoration of Atmospherically Degraded Images, Vol. 2, Woods Hole Summer Study, NAS/NRC, 1966.
2. H. T. Yura, Applied Optics, **12**, 1188 (1973).
3. L. I. Goldfischer, JOSA, **55**, 247 (1965).
4. M. Greenebaum and M. King (to be published).
5. V. I. Tatarskii, The Effects of the Turbulent Atmosphere on Wave Propagation, IPST Cat. No. 5319, Jerusalem, 1971.
6. R. S. Lawrence and J. W. Strohbehn, Proc. IEEE **58**, 1523 (1970).
7. J. R. Kerr, JOSA, **62**, 1040 (1972).
8. R. S. Lawrence, JOSA, **62**, 701L (1972).
9. M. King, M. Greenebaum, and M. Elbaum, Proc. 1974 Intl. Opt. Comp. Conf., Zürich, 1974 (to be published).
10. S. F. Clifford, G. R. Ochs, and R. S. Lawrence, JOSA, **64**, 148 (1974).
11. J. A. Dowling and P. M. Livingston, JOSA, **63**, 846 (1973).



ASSUME :

1. OBJECT LIES IN A SINGLE ISOPLANATIC REGION.
2. "UPLINK" AND "DOWNLINK" CAN BE TREATED SEPARATELY.
3. OBJECT CONSISTS OF INDEPENDENT, DIFFUSE SCATTERERS, WITH RANDOM PHASE AND $\sigma_s > \lambda$.

THEN THE INSTANTANEOUS IRRADIANCE RECEIVED IS :

$$I(\bar{p}') = I_1(\bar{p}') I_2(\bar{p}') I_3(\bar{p}')$$

$$= \overline{I(\bar{p}')} \prod_{m=1}^3 \left[1 + \frac{I_m(\bar{p}') - \overline{I_m(\bar{p}')}}{\overline{I_m(\bar{p}')}} \right]$$

where the three independent factors relate to:

- TURBULENCE FROM TRANSMITTER TO OBJECT (I_1),
- SCATTER FROM OBJECT IN ABSENCE OF TURBULENCE (I_2),
- and TURBULENCE FROM OBJECT TO RECEIVER (I_3).

THEN THE COVARIANCE OF THE RECEIVED IRRADIANCE IS:

$$\begin{aligned}
 C_1(\bar{\rho}) &= \frac{\langle [I(\bar{p}') - \overline{I(\bar{p}')}][I(\bar{p}'+\bar{\rho}) - \overline{I(\bar{p}'+\bar{\rho})}] \rangle}{\overline{I(\bar{p}')} \overline{I(\bar{p}'+\bar{\rho})}} \\
 &= C_1(\bar{\rho}) + C_2(\bar{\rho}) + C_3(\bar{\rho}) \\
 &\quad + C_1(\bar{\rho}) C_2(\bar{\rho}) + C_2(\bar{\rho}) C_3(\bar{\rho}) + C_3(\bar{\rho}) C_1(\bar{\rho}) \\
 &\quad + C_1(\bar{\rho}) C_2(\bar{\rho}) C_3(\bar{\rho}),
 \end{aligned}$$

where

$$C_m(\bar{\rho}) = \frac{\langle [I_m(\bar{p}') - \overline{I_m(\bar{p}')}][I_m(\bar{p}'+\bar{\rho}) - \overline{I_m(\bar{p}'+\bar{\rho})}] \rangle}{\overline{I_m(\bar{p}')} \overline{I_m(\bar{p}'+\bar{\rho})}},$$

$m = 1, 2, 3.$

As the notation indicates, we shall assume spatial stationarity, i. e., the covariances C_m depend on $\bar{\rho}$, not on position in the receiver aperture, \bar{p}' .

SCATTER FROM OBJECT IN ABSENCE OF TURBULENCE (I_2):

$C_2(\bar{\rho})$ = SPECKLE COVARIANCE

EFFECTIVE WIDTH OF $C_2(\bar{\rho})$ = $\lambda z/L_t$

$S_2(\bar{f})$ = FOURIER TRANSFORM OF $C_2(\bar{\rho})$

= "CORRELOGRAM" OF OBJECT

$C_2(0)$ = 1 .

TURBULENCE FROM OBJECT TO RECEIVER (l_3):

$$C_3(\bar{\rho}) = \exp [4 C_p(\bar{\rho})] - 1 = C_1^s(\bar{\rho}) / \langle l \rangle^2 ,$$

where $C_p(\bar{\rho})$ = LOG-AMPLITUDE COVARIANCE FOR POINT SOURCE
AT LOCATION OF OBJECT.

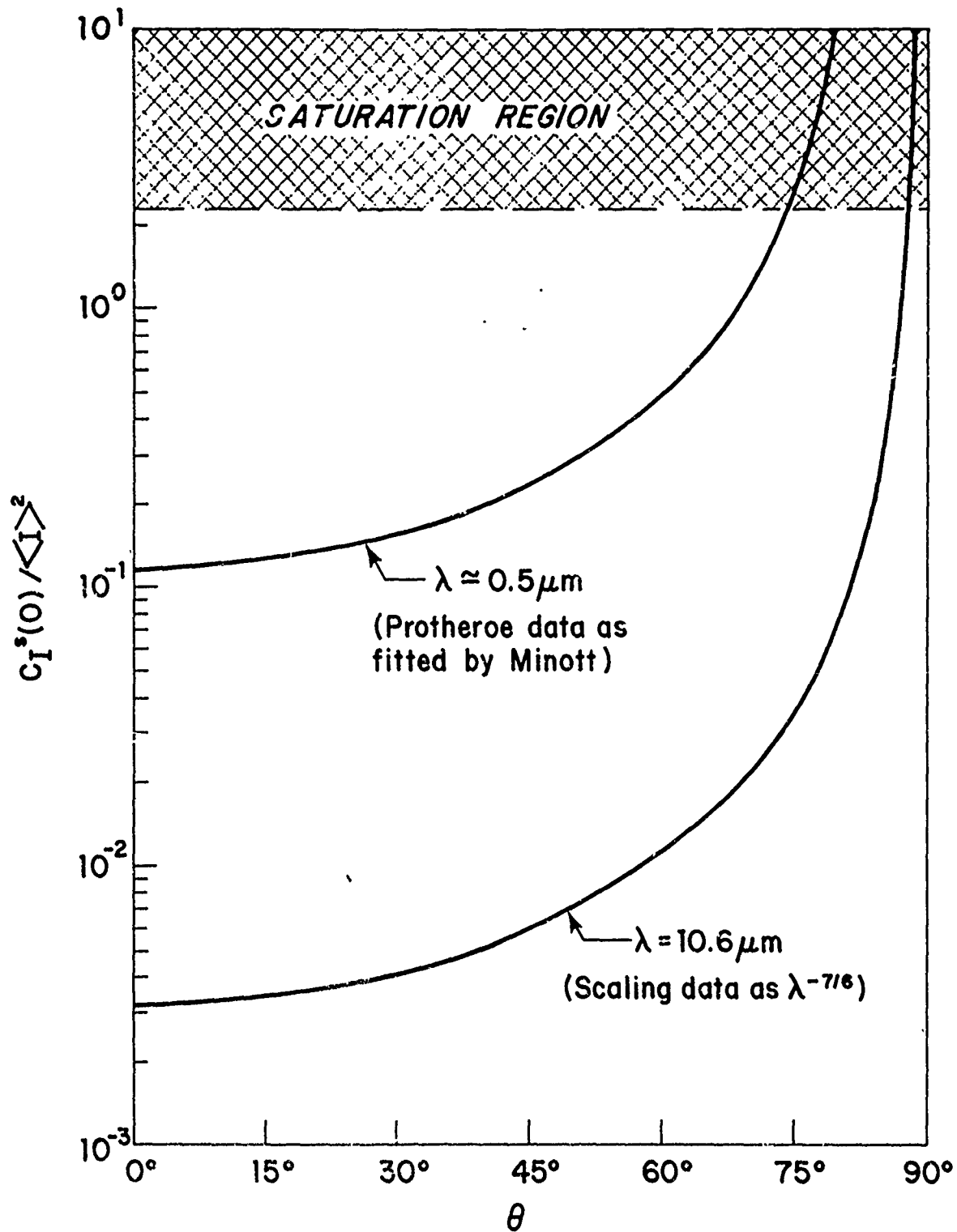
$$\begin{aligned} C_3(0) &= \text{STRENGTH OF RANDOM APODIZATION} \\ &= 0.12 \text{ at } \theta = 0^\circ \text{ at } 0.5 \mu\text{m} \\ &\quad 0.20 \text{ at } \theta = 40^\circ \\ &= 0.003 \text{ at } \theta = 0^\circ \text{ at } 10.6 \mu\text{m (CO}_2 \text{ LASER)} \\ &\quad 0.005 \text{ at } \theta = 40^\circ \end{aligned}$$

FOR $C_p(0) < 0.3$, NO PROBLEMS WITH "SATURATION".

Near-zenith estimates derived from stellar data of Protheroe, et al.
and scaled with wavelength as $k^{7/6}$:

$$\begin{aligned} C_p(0) &= 0.028 \text{ sec}^{11/6} \theta \quad (\text{VISIBLE REGION}) \\ &= 0.0008 \text{ sec}^{11/6} \theta \quad (\text{CO}_2 \text{ LASER}) \end{aligned}$$

$$\begin{aligned} \text{EFFECTIVE WIDTH OF } C_3(\bar{\rho}) &\approx \sqrt{\lambda h_0 \sec \theta} \quad (\text{no "saturation"}) \\ &= 4 \text{ to } 10 \text{ cm (VISIBLE REGION)} \\ &= 15 \text{ to } 45 \text{ cm (CO}_2 \text{ LASER)} \end{aligned}$$



TURBULENCE FROM TRANSMITTER TO OBJECT (I_1):

VARIANCE OF OBJECT ILLUMINATION IS LESS THAN $C_3(0)$
BECAUSE OF TRANSMITTER APERTURE-AVERAGING
(ASSUMING NO "SATURATION").

GENERALLY EXPECT $C_1(\bar{\rho}) \lesssim C_3(0)$.

EXPERIMENTAL VERIFICATION OF SCINTILLATION STRENGTH
(Minott, 1972).

$C_1(0)$ CAUSES DYNAMIC RANGE PROBLEM IN FOURIER-TRANSFORM
HOLOGRAPHY WITH PHOTOGRAPHIC FILM DETECTION
(Goodman, et al., 1968).

NEAR-HORIZONTAL PROPAGATION:

"SATURATION" REGION ENTERED AT LARGE ZENITH
ANGLES WHEN $C_1(0) \geq 0.3$.

THEN $1 = C_2(0) \ll C_3(0)$,

$C_3(\bar{\rho})$ ACQUIRES A RESIDUAL TAIL EXTENDING BEYOND $\sqrt{\lambda h_0 \sec \theta}$,

ANGULAR EXTENT OF ISOPLANATIC REGION SHRINKS WITH
INCREASING θ . (Yura, Clifford et al.)

EXPERIMENTAL DATA FROM STUDIES OF LENSLESS FOURIER-
TRANSFORM HOLOGRAPHY. (Goodman, Gaskill, et al.)

Example: For a 90-meter horizontal path, $\lambda = 0.6 \mu\text{m}$, linear
dimension of isoplanatic region is less than 5 cm.

SUMMARY

CAN EXTRACT OBJECT CORRELOGRAM (OR HOLOGRAPHIC IMAGE) FROM APERTURE-PLANE IRRADIANCE, EVEN WITH TURBULENCE, PROVIDED:

1. ANGULAR SUBTENSE OF OBJECT $\lesssim 10\mu\text{rad}$.
2. OBJECT ROTATION IS NEGLIGIBLE.
3. CO₂ LASER ILLUMINATION, DETECTOR ARRAY, EVEN AT LARGE ZENITH DISTANCES.
4. LONG-COHERENCE VISIBLE LASER, OBJECT VERY NEAR ZENITH.

VERIFICATION OF CONCEPT OVER NEAR-HORIZONTAL PATHS IS DIFFICULT.

ASSUMPTIONS: Rough Object ($\sigma_s > \lambda$)
 Independent Scattering Cells
 Huygens-Fresnel Principle
 Isoplanatic Approximation

INSTANTANEOUS FIELD AT RECEIVER:

$$\bar{E}(\bar{p}', t) = \sum_{i=1}^N \bar{E}_0(\bar{p}_i, t) G(\bar{p}_i, \bar{p}'),$$

where $\bar{E}_0(\bar{p}, t) \propto \tau(\bar{p}) I_0^{1/2}(\bar{p}, t) \exp iks(\bar{p})$,

$$G(\bar{p}_i, \bar{p}') = G_0(\bar{p}_i, \bar{p}') \exp[\mathcal{I}(\bar{p}_i, \bar{p}') + i\phi^a(\bar{p}_i, \bar{p}')] ,$$

$I_0(\bar{p}, t)$ = illumination at wavelength $\lambda = 2\pi/k$,

$\tau(\bar{p})$ = local diffuse reflection coefficient,

$s(\bar{p})$ = random surface depth variable,

$G_0(\bar{p}_i, \bar{p}') = z^{-1} \exp ikz(\bar{p}_i, \bar{p}') =$ Green's function with no turbulence,

$\mathcal{I}(\bar{p}_i, \bar{p}')$ = turbulence-induced log-amplitude perturbation,

$\phi^a(\bar{p}_i, \bar{p}')$ = turbulence-induced phase perturbation.

$$\phi^a(\bar{p}_i, \bar{p}') - \phi^a(\bar{p}_j, \bar{p}') = \phi^a(\bar{p}_i, \bar{p}' + \bar{\rho}) - \phi^a(\bar{p}_j, \bar{p}' + \bar{\rho}) , \quad (\text{ISOPLANATISM})$$

$$\mathcal{I}(\bar{p}_i, \bar{p}') = \mathcal{I}(\bar{p}_j, \bar{p}') = \mathcal{I}(\bar{p}, \bar{p}')$$

NOTE: IN F-T HOLOGRAPHY, $\tau(\bar{p}_{ref})$ = specular reflectance,

$$s(\bar{p}_{ref}) = 0.$$

RIVERSIDE RESEARCH INSTITUTE

Paper No. 5

COMPUTATIONS OF SIGNAL-TO-NOISE RATIO IN CORRELOGRAPHY

This paper⁵ was originally written in response to an erroneous calculation of signal-to-noise ratio in laser correlography which was performed by the Hughes Research Laboratories. The Hughes claim had been that "more than 10,000 pulses would have to be averaged to obtain adequate signal-to-noise ratio" in laser correlography.¹⁶ In this paper,⁵ it is shown that only 20 "looks" suffice to obtain adequate signal-to-noise ratio, rather than 10,000. Subsequent laboratory demonstration experiments have amply verified the signal-to-noise calculation given here, as documented in a forthcoming RRI Technical Report.¹⁵

RIVERSIDE RESEARCH INSTITUTE



80 West End Avenue / New York, New York 10023 / (212) 873-4000

15 March 1974

RESEARCH NOTE N-1/306-3-11

COMPUTATIONS OF SIGNAL-TO-NOISE RATIO IN CORRELOGRAPHY

Prepared for

Director

Defense Advanced Research Projects Agency

1400 Wilson Boulevard

Arlington, Virginia 22209

Contract No.: DAAH01-74-C-0419

Prepared by:

Marek Elbaum

Approved by:

M. King
M. King, Manager,
Optics Laboratory

RIVERSIDE RESEARCH INSTITUTE

INTRODUCTION

In this note we shall comment on the computation of the signal-to-noise ratio for correlography performed at Hughes Research Laboratories¹. Specifically, we show that their discouraging results calling for 10,000 laser pulses to obtain adequate S/N ratio at the spatial frequencies of interest, arises from a poor choice of the processing used to estimate the autocorrelation function of the speckle pattern. (These Hughes predictions were obtained under the assumptions that the speckle patterns are unperturbed by the atmospheric turbulence, and that the illumination energy is large enough that shot noise is negligible.)

In the following, we briefly review the principles on which correlography is based, emphasizing the availability of two modes of processing of the information, i.e.: (1) estimation of the correlation function of the speckle pattern, and (2) the estimation of the power spectrum of the speckle pattern. The statistical properties of several estimators are used to argue that there exist statistics which can be used to extract intelligence about the object when no more than twenty laser pulses are used.

THE SPECKLE PATTERN

A coherently illuminated object with an optically rough surface generates a speckle pattern. This speckle pattern, which represents a stochastic process over the plane of the receiver, is the "signal" used in correlography. It is well-known that:

- 1) The autocorrelation function of the speckle pattern yields the absolute square amplitude of the Fourier transform of the object irradiance distribution.
- 2) The power spectral density of the speckle pattern yields the autocorrelation function of the object irradiance distribution (correlogram).

In practice, the speckle pattern $I(u,v)$ is available only across a finite receiver aperture, and the number of independent realizations of this pattern (obtained from a series of laser illumination pulses) is limited. Therefore, correlography is a technique in which the information about the object is derived from estimators of either the correlation function or of the power spectral density of the speckle pattern. In correlography, the choice of the optimal processing method must depend on the statistical properties of these estimators.

CORRELATION FUNCTION ESTIMATORS

The statistic used by researchers from Hughes to estimate the correlation function of the speckle pattern is defined as:

$$(1) C_1(\delta u, \delta v) = \frac{1}{M} \sum_{n=1}^M (I^{(n)}(u, v) - \bar{I}) (I^{(n)}(u - \delta u, v - \delta v) - \bar{I}),$$

where M is the number of independent realizations of the speckle pattern measured by a single pair of detectors separated by the distance $(\delta u, \delta v)$. The mean irradiance, \bar{I} , is taken as constant across the pair, i. e., $\bar{I} = E [I(u, v)] = E [I(u - \delta u, v - \delta v)]$.

The signal-to-noise ratio is defined as the ratio of the expected value of C_1 to the standard deviation of C_1 , and is equal to

$$(2) \left(\frac{S}{N}\right)_{C_1} \triangleq \frac{E(C_1)}{\text{Var}(C_1)} \sim \sqrt{M} \frac{C(\delta u, \delta v)}{\bar{I}^2}^*$$

where $C(\delta u, \delta v)$ is the true value of the correlation function.

We observe that if the speckle pattern has a negative-exponential probability density function (for which the standard deviation is equal to the mean), $\frac{C(\delta u, \delta v)}{\bar{I}^2} \leq 1$ for all values of $(\delta u, \delta v)$.

* Formula v-48, used to compute S/N in the HRL report¹ (p. 123), is the square of equation (2) and may be considered equivalent to it. The reason for the apparent difference stems from the fact that v-48 considers power ratio at the output of an electronic processor, whereas our formulae (2), (4) and (6) express amplitude S/N ratios for an electronic processor.

Instead of the statistic C_1 , it is more advantageous to introduce the statistic C_2 , which can be realized by scanning the irradiance distribution across the entire receiver aperture, and which is defined as

$$(3) \quad C_2(\delta u, \delta v) = \frac{1}{A} \cdot \frac{1}{A} \sum_{n=1}^M \iint_A \left[\left(I^{(n)}(u, v) - \bar{I} \right) \left(I^{(n)}(u - \delta u, v - \delta v) - \bar{I} \right) \right] du dv,$$

where A is the area of the receiver. The signal-to-noise ratio is defined as before, i.e., as a ratio of the expected value of C_2 to its standard deviation. In the particular case of a circular Gaussian autocorrelation of the speckle irradiance, for example, signal-to-noise is given by

$$(4) \quad \left(\frac{S}{N} \right)_{C_2} \sim \sqrt{M} \sqrt{\frac{A}{\text{Speckle size}}} e^{-2h^2/h_0^2} = \sqrt{M} \sqrt{\frac{A}{\text{Speckle size}}} \frac{C(\delta u, \delta v)}{\bar{I}^2},$$

where it is assumed that the true value of the correlation function, C , is given by

$$C = \bar{I}^2 e^{-2h^2/h_0^2},$$

where $h^2 = \delta u^2 + \delta v^2$

and $h_0/\sqrt{2}$ is the $1/e$ width of the correlation function.

Comparing the statistics C_1 and C_2 , we observe that although both are unbiased estimators of the correlation function C , only the second one is a consistent estimator. Thus, as the aperture of the receiver, A , increases, C_2 tends to be clustered about the ensemble average.

The signal-to-noise ratio computed for C_2 is superior by a factor $\sqrt{\frac{A}{\text{Speckle area}}}$ with respect to that computed for C_1 . For a 5-m-diameter target at a distance of 400 km from the ground-based receiver, illuminated with 0.5 μm laser light, and observed with a receiver of 1 -m aperture diameter, this factor is on the order of 25! (or 625 when the square of the Eq 4 is compared with formula v.48).

POWER SPECTRAL DENSITY ESTIMATORS

Based on rough analytical predictions^{2,3}, and as supported by laboratory demonstrations at RRI⁴, we have found that the power spectral estimators of the speckle pattern have even more useful properties, and are likely to be the optimal statistics for correlography.

One such statistic, which has been used successfully to obtain an adequate signal-to-noise ratio with less than twenty independent samples of the speckle pattern, is defined as

$$(5) \quad S_1(f_u, f_v) = \frac{1}{M} \cdot \frac{1}{A} \sum_{n=1}^M \left| \iint_A I^{(n)}(u, v) e^{-i2\pi(f_u u + f_v v)} du dv \right|^2$$

The signal-to-noise ratio computed for this statistic is equal to

$$(6) \quad \left(\frac{S}{N}\right)_{S_1} = \frac{E[S_1]}{(\text{Var}S_1)^{1/2}} = \sqrt{M}$$

RIVERSIDE RESEARCH INSTITUTE

at any spatial frequency "resolvable" by the receiver aperture A. In deriving the last equation, it has been assumed that the estimator S_1 , has a chi-square distribution^{2,3} with two degrees of freedom (for which the mean is equal to the standard deviation). For $M = 20$, the signal-to-noise is equal to 4.5 for all arguments of the power spectrum estimator.

REFERENCES

1. Bridges, W. B., Brown, W. P., Jr., Jenney, J. A., O'Meara, T. R., Pedinoff, M. E., and Tseng, D. Y., "Space Object Imaging Techniques," Semiannual Technical Report, Hughes Research Laboratories, Malibu, Cal., Contract DAAH01-73-C-0629, November 1973.
2. Bendat, J. S., Piersol, A. G., "Measurement and Analysis of Random Data," John Wiley & Sons, New York, 1966.
3. Jenkins, G. M., and Watts, D. G., "Spectral Analysis and Its Applications," Holden-Day 1969, San Francisco, p.417.
4. King, M., Greenebaum, M., Elbaum, M., "Influence of the Atmosphere on Laser Produced Speckle Patterns," Proceedings of 1974 International Optical Computing Conference (Zurich, Switzerland), 1974, to be published.

RIVERSIDE RESEARCH INSTITUTE

Paper No. 6

PRELIMINARY PLAN FOR A LASER CORRELOGRAPHY EXPERIMENT

(This paper is a slightly edited version of RRI Research Note N-2/174-3-35.² It describes the design of a feasibility demonstration experiment, using coherent ruby-laser illumination of suitable space objects, and designed around a more-or-less conventional telescope facility. It is in the form of Vu-Graphs, with commentary on facing pages, and expands upon some of the issues discussed in Sections II A and B of Paper No. 1.)

RIVERSIDE RESEARCH INSTITUTE

The purposes of this experiment are threefold. First and primary is the demonstration of the feasibility of this technique for obtaining correlograms of orbiting space vehicles. Second, a meaningful opportunity to assess the practical utility of such signatures will arise from successful completion of the experiment. Finally, several aspects of laser correlography system design may be confirmed by the experimental results. These include the influences of glint, target motion, atmospheric apodization and choice of optimum signal processing.

PURPOSE OF LASER CORRELOGRAPHY EXPERIMENT

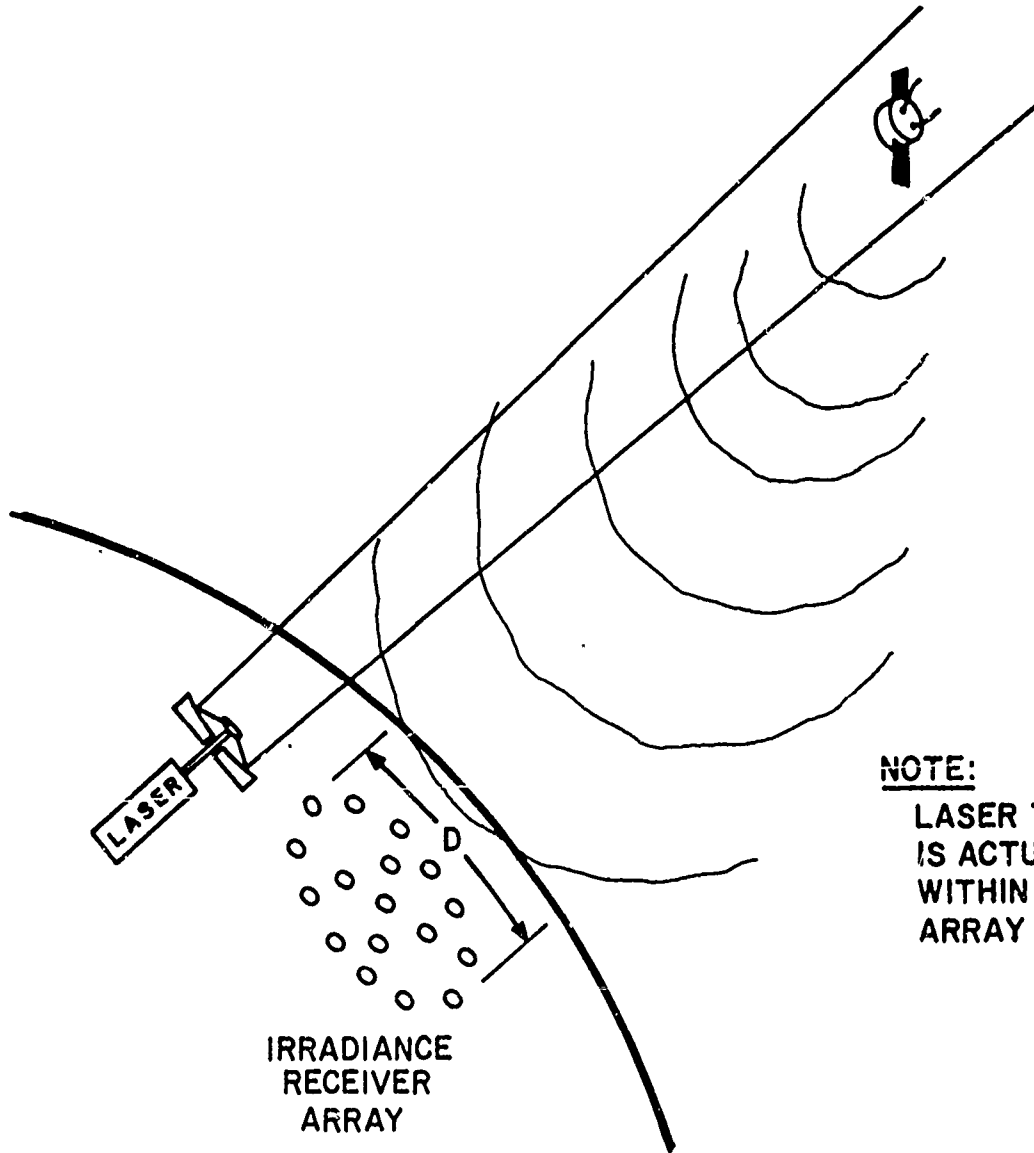
- FEASIBILITY DEMONSTRATION
- SIGNATURE EVALUATION / INTERPRETATION
- SYSTEM DESIGN CONFIRMATION
 - GLINT VS. DIFFUSE TARGETS
 - ATMOSPHERIC EFFECTS
 - TARGET MOTION
 - SIGNAL PROCESSING

RIVERSIDE RESEARCH INSTITUTE

This figure shows the basic elements of a laser correlography system configuration. A ground-based laser illuminates a space vehicle; the backscattered laser light forms a self-interference pattern which is sampled by the irradiated receiver array. It is expected that the structural nature* of this pattern, which is related to the shape, size and structure of the target, will survive passage through the relatively thin turbulent atmospheric layer.

* More precisely, the two-dimensional power spectrum of the pattern. See Paper No. 3 for the gory details, which demonstrate that this power spectrum is proportional to the correlogram of the target.

FIG. 1 LASER CORRELOGRAPHY SYSTEM



NOTE:
LASER TRANSMITTER
IS ACTUALLY PLACED
WITHIN RECEIVER
ARRAY AREA

RIVERSIDE RESEARCH INSTITUTE

A laser correlogram is the autocorrelation of the image of the object. Such signatures should be useful for measurement of various object dimensions as well as the identification of features on targets and entire target systems. Resolution is expected to be limited almost totally by receiving aperture size with minor degradation in the visible region where the proposed feasibility experiment will be performed. Finally, it should be noted that several looks or returns are required from a single target aspect in order to obtain measures of the average speckle structure; our results have shown thirty looks to be adequate for reducing the variability of the signature. (See Paper No. 5.)



RIVERSIDE RESEARCH INSTITUTE

T-1/306-3-11

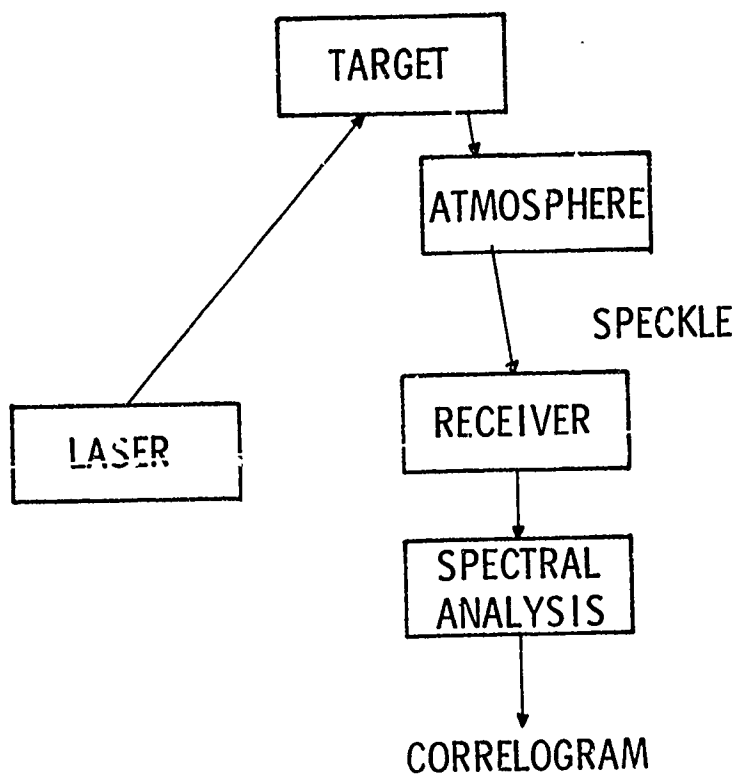
PROPERTIES OF LASER CORRELOGRAMS

- IMAGE CORRELATION
MENSURATION
FEATURE IDENTIFICATION
TARGET IDENTIFICATION
- λ/D RESOLUTION
MINOR ATMOSPHERIC DEGRADATION
AT $0.7 \mu\text{m}$
- REQUIRES SEVERAL LOOKS PER TARGET ASPECT
AVERAGE SPECKLE STRUCTURE
30 FRAMES ADEQUATE

RIVERSIDE RESEARCH INSTITUTE

This block diagram shows the essential elements that must be specified in order to describe the laser correlography experiment.

BLOCK DIAGRAM OF LASER
CORRELOGRAPHY SYSTEM



RIVERSIDE RESEARCH INSTITUTE

For the purpose of experimental design, the target was assumed to be described by the parameters of the accompanying figure. Also, atmospheric seeing of better than 2 arc seconds and transmission loss of 1.5 dB were assumed.

SYSTEM SPECIFICATIONS

Target

- 3m maximum dimension, 10m² area
- Diffuse Reflectivity 0.1
- Target Range - 350 km
- Earth Stabilized
- Duration of Pass - 2 min (nominal)

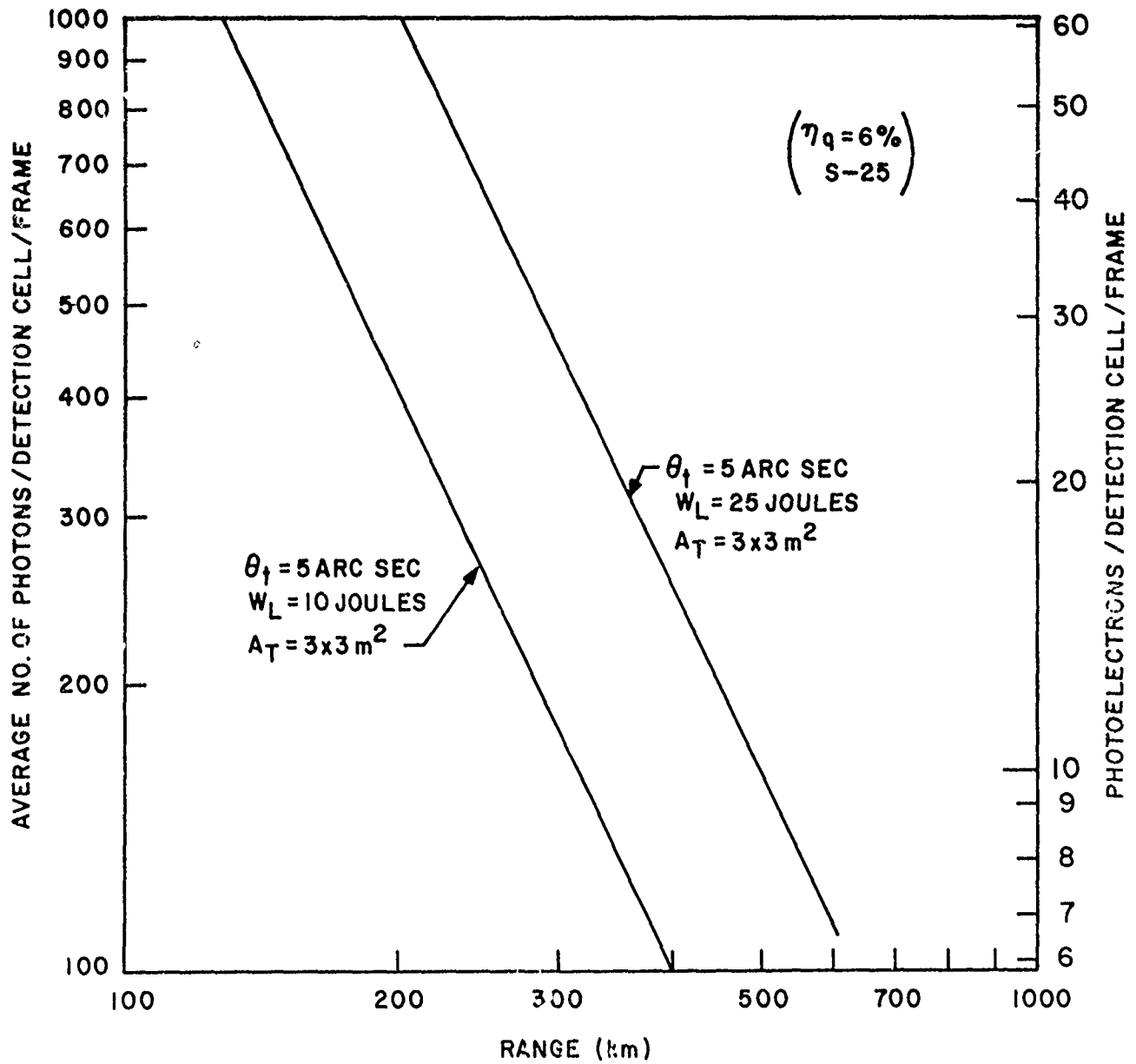
Environment

- Seeing $\approx 2''$
- Atmospheric two-way loss = 1.5 dB at 0.7 μ m

RIVERSIDE RESEARCH INSTITUTE

This graph plots the average return as a function of target range for 10- and 25-joule laser pulses directed in 5 arc second beam widths at targets described above. The left-hand ordinate shows the average number of photons arriving per detection cell per transmit pulse; the right-hand ordinate reduces this number according to the 6% quantum efficiency of an S-25 photocathode. In each case, the area of a detection cell is equal to one-fourth the area of the smallest speckle in the backscatter pattern. Note that a 10-joule pulse directed at a target at 350-km range provides 8.5 photoelectrons per detection cell. It is expected that the actual laser energy per pulse will lie somewhere between the 10 and 25 joule curves shown.

AVERAGE RETURN VS TARGET RANGE



RIVERSIDE RESEARCH INSTITUTE

As a result of this calculation, the laser illuminator specification expressed in the accompanying chart is obtained. A nominal 10-joule/pulse ruby transmitter is specified, and the required coherence length of 10 meters allows for 5-meter target depth.

SYSTEM SPECIFICATIONS (Cont'd)

Correlography Illuminator

- 0.7 μ m
- 10 joules / pulse
- ~ 100 nsec pulse width
- 20 pulses / minute - repetition rate
- Coherence length - 10 meters
- Illuminator beamwidth - 5 arcsec

RIVERSIDE RESEARCH INSTITUTE

Also, as a result of the above calculation, the receiver intensity detector must be signal shot noise limited and our studies show that this can be achieved with a dynamic range of 25 dB using a SIT or EBS tube preceded by an image intensifier.

SYSTEM SPECIFICATIONS (Cont'd)

Correlography Receiver

Image Tube

- Electronic Range Gate - 1 msec
- S-25 Photocathode ($\eta \sim 6\%$)
- Isocon Intensifier / SIT or EBS
- Dynamic Range ~ 25 dB

Signal Shot Noise Limited Detection

RIVERSIDE RESEARCH INSTITUTE

Finally, the output resulting from, e. g., a two-minute satellite pass will be 30 to 50 frames of data with target resolution of 20 cm and a signal-to-noise ratio of ~ 3 . During a two-minute pass, it is necessary that the target have a nearly constant range and small rotation; such targets are available.

CORRELOC. RAM OUTPUT

ONE SATELLITE PASS (~ 2 minutes)

TARGET RESOLUTION	20 cm
FRAMES OF DATA	30 TO 50
SIGNAL TO NOISE RATIO	3

RIVERSIDE RESEARCH INSTITUTE

REFERENCES*

1. King, M., "Laser SOSI Technology (U)," Secret, Research Note N-5/174-3-33, Riverside Research Institute, New York, N. Y., 21 August 1972.
2. King, M., "Preliminary Plan for a Laser Correlography Experiment (U)," Unclassified, Research Note N-2/174-3-35, Riverside Research Institute, New York, N. Y., 18 May 1973.
3. Greenebaum, M., "Near-Zenith Estimates of Random Apodization at 10.6 μm (U)," Unclassified, Research Note N-6/174-3-33, Riverside Research Institute, New York, N. Y., 15 November 1972.
4. Greenebaum, M. and M. King, "Laser-Produced Speckle Patterns as Seen Through a Randomly Inhomogeneous Atmosphere (U)," Unclassified, Research Note N-8/174-3-33, Riverside Research Institute, New York, N. Y., 28 November 1972. Reissued with minor revisions under same title as PTP-100, 25 June 1973, and as PTP-100(R), 21 December 1973.
5. Elbaum, M., "Computations of Signal-to-Noise Ratio in Correlography (U)," Unclassified, Research Note N-1/306-3-11, Riverside Research Institute, New York, N. Y., 15 March 1974.
6. King, M., M. Greenebaum, and M. Elbaum, "Influence of the Atmosphere on Laser Produced Speckle Patterns," Digest of Papers Presented at the 1974 International Optical Computing Conference, April 9-11, 1974, Zürich, Switzerland, Institute of Electrical and Electronics Engineers, Inc., New York, N. Y. (IEEE Catalog No. 74 CH0862-3C), pp. 64-68.
7. Greenebaum, M., "The Residual Effects of Atmospheric Turbulence on a Class of Holographic Imaging and Correlography Systems," Digest of Technical Papers, Topical Meeting on Optical Propagation Through Turbulence, July 9-11, 1974, University of Colorado, Boulder, Colo., Paper Th A6. (Available from Optical Society of America, Washington, D. C.)
8. Goodman, J. W., D. W. Jackson, M. Lehmann, and J. W. Knotts, "Holographic Imagery Through Atmospheric Inhomogeneities," in Evaluation of Motion-Degraded Images, NASA SP-193, U. S. Government Printing Office, Washington,

RIVERSIDE RESEARCH INSTITUTE

- D. C., 1969, pp. 123-127.
9. Gaskill, J. D., "Imaging Through a Randomly Inhomogeneous Medium by Wavefront Reconstruction," *J. Opt. Soc. Amer.*, 58, 600-608 (1968); "Atmospheric Degradation of Holographic Images," *J. Opt. Soc. Amer.*, 59, 308-318 (1969).
 10. Yura, H. T., "Holography in a Random Spatially Inhomogeneous Medium," *Applied Optics*, 12, 1188-1192 (1973).
 11. Goldfischer, L. I., "Autocorrelation Function and Power Spectral Density of Laser-Produced Speckle Patterns," *J. Opt. Soc. Amer.*, 55, 247-253 (1965).
 12. Bulabois, J., M. E. Guillaume, and J. Ch. Viénot, "Applications of the Speckle Pattern Techniques to the Visualization of Modulation Transfer Functions and Quantitative Study of Vibrations of Mechanical Structures," *Applied Optics*, 12, 1686-1692 (1973).
 13. Everett, P. N., and A. J. Cantor, "Long-Range Holography," *Applied Optics*, 11, 1697-1707 (1972).
 14. Deitz, P. H., "An Experimental Comparison of Imagery by Means of Spatial Intensity Interferometry and Standard Techniques," *Digest of Technical Papers, Topical Meeting on Optical Propagation Through Turbulence, July 9-11, 1974*, University of Colorado, Boulder, Colo., Paper Th A8. (Available from Optical Society of America, Washington, D. C.)
 15. King, M., L. Schlom, and W. Edelson, "Laser Correlography: System Simulations (U)," *Unclassified, Technical Report T-2/306-3-11*, Riverside Research Institute, New York, N. Y., in preparation.
 16. Bridges, W. B., W. P. Brown, Jr., J. A. Jenney, T. R. O'Meara, M. E. Pedinoff, and D. Y. Tseng, "Space Object Imaging Techniques (U)," *Semiannual Technical Report*, Hughes Research Laboratories, Malibu, CA, Contract DAAH01-73-C-0629, November 1973, p. 123. See also Ref. 17.
 17. Bridges, W. B., W. P. Brown, Jr., J. A. Jenney, T. R. O'Meara, M. E. Pedinoff, and D. Y. Tseng, "Space Object Imaging Techniques (U)," *Final Technical Report 13 March 73-31 Dec 73*, Hughes Research Laboratories, Malibu, CA, Contract No. DAAH01-73-C-0629, June 1974, pp. 223-224.

* Papers No. 2 through 5 are self-contained and include their own references. Only the references cited in the remainder of this Technical Report refer to this list.

UNCLASSIFIED

SECURITY CLASSIFICATION OF THIS PAGE (When Data Entered)

REPORT DOCUMENTATION PAGE		READ INSTRUCTIONS BEFORE COMPLETING FORM
1. REPORT NUMBER	2. GOVT ACCESSION NO.	3. RECIPIENT'S CATALOG NUMBER
4. TITLE (and Subtitle) (E) LASER CORRELOGRAPHY: TRANSMISSION OF HIGH-RESOLUTION OBJECT SIGNATURES THROUGH THE TURBULENT ATMOSPHERE,		5. TYPE OF REPORT & PERIOD COVERED (9) Technical Report,
7. AUTHOR(s) (10) M. Elbaum, Mo/King and M. Greenebaum		6. PERFORMING ORG. REPORT NUMBER T-1/306-3-11
9. PERFORMING ORGANIZATION NAME AND ADDRESS Riverside Research Institute 80 West End Avenue New York, N. Y. 10023		8. CONTRACT OR GRANT NUMBER(s) (15) DAAH01-74-C-0419 ARPA Order-2287
11. CONTROLLING OFFICE NAME AND ADDRESS Advanced Research Projects Agency Arlington, Virginia 22209		10. PROGRAM ELEMENT, PROJECT, TASK AREA & WORK UNIT NUMBERS (12) 120p.
14. MONITORING AGENCY NAME & ADDRESS (if different from Controlling Office) U. S. Army Missile Command Redstone Arsenal, Alabama 35809		13. REPORT DATE (11) 31 October 1974
16. DISTRIBUTION STATEMENT (of this Report) (14) BRI-T-1/306-3-11 Approved for public release; distribution unlimited.		14. NUMBER OF PAGES 122
17. DISTRIBUTION STATEMENT (of the abstract entered in Block 20, if different from Report)		15. SECURITY CLASS. (of this report) Unclassified
18. SUPPLEMENTARY NOTES		15a. DECLASSIFICATION/DOWNGRADING SCHEDULE
19. KEY WORDS (Continue on reverse side if necessary and identify by block number) Laser correlography Random apodization Correlation functions Signal to noise ratio Holographic imaging Infrared optical systems Atmospheric scintillation Optical radar Laser speckle		
20. ABSTRACT (Continue on reverse side if necessary and identify by block number) A correlogram is the two-dimensional autocorrelation of the image of an object illuminated with non-coherent radiation. A laser correlogram is obtained from the power spectrum of the irradiance pattern scattered from the object when illuminated with sufficiently coherent radiation. The resolution of this signature is dictated by the size of the receiving aperture, with relatively minor degradation by atmospheric		

UNCLASSIFIED

SECURITY CLASSIFICATION OF THIS PAGE(When Data Entered)

turbulence. This report collects in one place information which has been available up to now only in conference proceedings or in limited-circulation Research Notes of the Riverside Research Institute. The subjects treated analytically include: a model for laser backscattering, studies on the influence of atmospheric turbulence on the laser correlogram, statistical convergence properties of the laser correlogram signature, qualitative experimental laboratory results, and the outline of a design for a ruby-laser experiment using space objects.

UNCLASSIFIED

SECURITY CLASSIFICATION OF THIS PAGE(When Data Entered)